Heliyon 10 (2024) e35955

Contents lists available at ScienceDirect

Heliyon

journal homepage: www.cell.com/heliyon

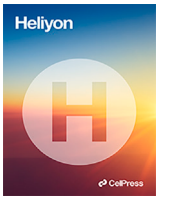

Research article

New computations of the fractional worms transmission model in wireless sensor network in view of new integral transform with statistical analysis; an analysis of information and communication technologies

Saima Rashid [a,*], Rafia Shafique [a,*], Saima Akram [b,c], Sayed K. Elagan [d]

[a] Department of Mathematics, Government College University, Faisalabad 38000, Pakistan
[b] Department of Mathematics, Government College for Women University Faisalabad, Faisalabad 38000, Pakistan
[c] Centre for Advanced Studies in Pure and Applied Mathematics, Bahauddin Zakariya, Multan 60000, Pakistan
[d] Department of Mathematics and Statistics, College of Science, Taif University, P.O. Box 11099, Taif 21944, Saudi Arabia

ARTICLE INFO

MSC:
26A51
26A33
26D07
26D10
26D15

Keywords:
Worm transmission model
Wireless sensor network
Technology adoption
Social media network
Homotopy perturbation method
$\mathcal{ZZ}$-transform
Atangana-Baleanu fractional derivative
Stability
Existence and uniqueness

ABSTRACT

Wireless sensor networks (WSNs) have attracted a lot of interest due to their enormous potential for both military and civilian uses. Worm attacks can quickly target WSNs because of the network's weak security. The worm can spread throughout the network by interacting with a single unsafe node. Moreover, the analysis of worm spread in WSNs can benefit from the use of mathematical epidemic models. We suggest a five-compartment model to characterize the mechanisms of worm proliferation with respect to time in WSN. Taking into account the $\mathcal{ZZ}$ transform convoluted with the Atangana-Baleanu-Caputo (ABC) fractional derivative operator, we employ it to analyze the characteristics and applications of the $\mathcal{ZZ}$ transformation using the Mittag-Leffler kernel. Moreover, we construct a new algorithm for the homotopy perturbation method (HPM) in conjunction with the $\mathcal{ZZ}$ transform technique to generate analytical solutions for the worm transmission model. Also, we address the qualitative aspects such as positivity, boundness, worm-free state, endemic state, basic reproduction number ($\mathcal{R}_0$) and worm-free equilibrium stability. Furthermore, we prove that the virus rate in sensor nodes is extinct if $\mathcal{R}_0 < 1$ and the virus persists if $\mathcal{R}_0 > 1$. In addition, we develop analytical findings to evaluate the series of solutions. Furthermore, a detailed statistical analysis is conducted to verify the nonlinear dynamics of the system by verifying the $0-1$ test to determine whether uncertainty exists using approximation entropy and the $\mathbb{C}_0$ data. An extensive analysis of the vaccination class with respect to the transmitting class as well as the susceptible class is being used to investigate the effects of stepping up precautions on WP in WSN. Moreover, the modeling of the WSN revealed that reducing the fractional-order from 1 requires that the recommended approach be implemented at the highest rate so that there is no long-lasting immunization; instead, nodes remain briefly defensive before becoming vulnerable to future worm attacks.

* Corresponding authors.
E-mail addresses: saimarashid@gcuf.edu.pk (S. Rashid), rafiasch2195@gmail.com (R. Shafique), saimaakram@gcwuf.edu.pk (S. Akram), skhalil@tu.edu.sa (S.K. Elagan).

https://doi.org/10.1016/j.heliyon.2024.e35955
Received 14 January 2024; Received in revised form 28 July 2024; Accepted 6 August 2024

Available online 13 August 2024

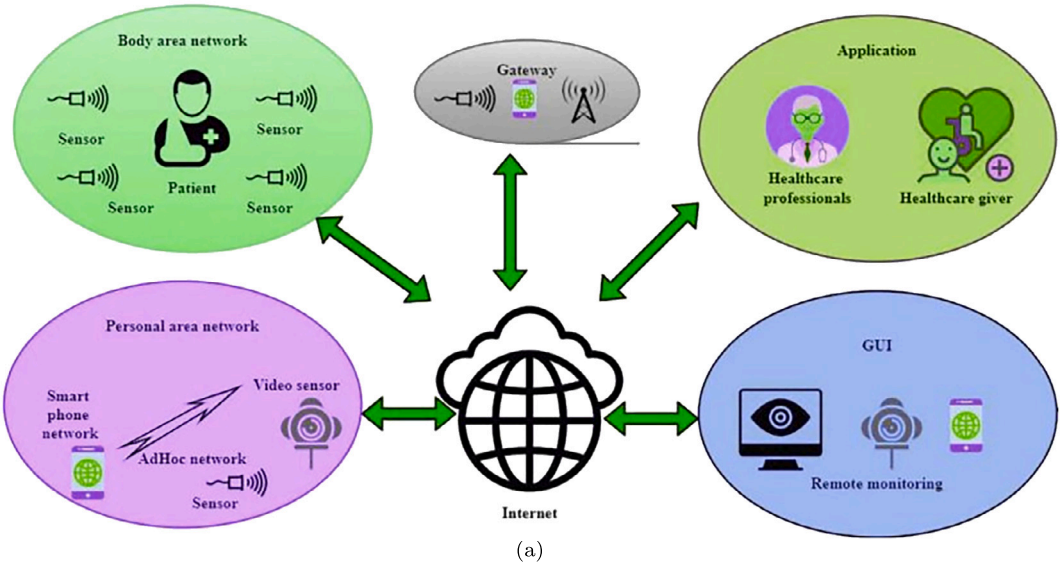

(a)

Fig. 1. Situation in which the propagation of worm in WSN model (3.1) is used.

1. Introduction

Recently, a worms propagation (WP) might have included hundreds or thousands of sensor nodes. Although it first emerged to provide support in military operations, its usage has now spread to multiple consumer and business markets, including traffic, health, and hence forth. The equipment for the sensor node consisted of an antenna-equipped radio transceiver, a microcontroller, a circuit of electricity for the interface, and an energy source, generally a battery, (see Fig. 1). The sensor nodes' dimensions can also vary in size, ranging from that of a shoe box to that of a dust element. Because of this, expenses also differ, ranging from just a few cents to hundreds of dollars, according to the technical characteristics of a sensor, such as memory, bandwidth, and processing rate [1]. One type of wireless network is a WSN, which involves a large number of moving, autonomous, small, lightweight, low-powered devices known as sensor nodes or motes. These networks undoubtedly encompass a vast array of tiny, battery-powered, embedded, geographically dispersed devices that are networked to meticulously gather, process, and provide the operators access to data, and they have managed the processing and computational capacities. The minor computers, known as nodes, combine to establish networks [2]. The wireless node for sensors is a multipurpose, energy-efficient instrument. Motes are used extensively in manufacturing processes. Transceivers can be used to facilitate conversation across motels. Ad-hoc networks, in comparison to sensors, will consist of fewer nodes and therefore no structure.

A novel class of worms that attack portable computers, including laptops and smartphones, has emerged in recent years. One unique aspect of these worms is that they may spread without the need for internet access. Through the use of wireless communication technologies like Wi-Fi and Bluetooth, they can spread straight from device to device [3,4]. Malicious software that specifically targets wireless devices has indeed begun to surface. With its ability to spread over air interactions, the recently identified virus Cabir poses a fatal threat to WSNs. Malware that attacks WSNs will inevitably materialize. Similar detection techniques are employed by the Mabir virus to initiate accessibility attacks. The WSN population is consequently very interested in protection techniques that could protect monitoring networks against malware intrusions. Epidemic modeling for infection propagation can be used to study the behaviors of hazardous substances via a web [5]. On the basis of Kermark and McKendrick's SIR classical epidemic model, dynamic models for the spreading of dangerous materials are being suggested [6]. According to network features that account for the structural components of the system, these frameworks offer an evaluation of the time-varying modifications of contaminated networks [5,7]. This method was used to email propagation methods [8] and, by modifying SIR models, produced infection prevention guidelines using the epidemiological threshold idea [5,9]. The research team's suggested model, SEIR [10], makes the unrealistic assumption that recovered hosts have a fixed chance of a lifelong immunization phase. To get over this restriction, Mishra and Saini [7] provide an SEIRS model including latent and immunological phases that can show how common worms spread. In order to investigate the prevalence of viruses, additional research has recently focused on the integration of virus propagation models with antiviral defensive measures, such as virus vaccination and quarantine [11]. The epidemiological models that are widely utilized by social scientists [12] may be used in studying the spreading of viruses in wireless networks because there are fundamental similarities between the propagation of software viruses among wireless devices and the development of epidemic illnesses in a population. Recent work has examined a few relevant uses of epidemic models in wireless circumstances [13].

However, the application of fractional calculus (FC) brought revolutionary changes in real-world phenomena, such as by introducing new notions of derivative and integral operators with singular/non-singular and local/non-local kernels [14]. The unique element put forth makes use of the generalized Mittag-Leffler function (GMLF), which constitutes the cornerstone [15,16]. Abdeljawad and Baleanu [17] introduced the discrete fractional operators with nonsingular discrete Mittag-Leffler kernels. Therefore,

the properties of this mechanism exacerbate the novel formulations to achieve numerous intriguing characteristics, like the mean square deformation interphase and expanding variations, that have been discovered in serious unforeseen circumstances. It has been frequently utilized in many fields of science and technology since Atangana and Baleanu [18] presented the innovative fractional derivative operator in 2016. It has been demonstrated that using the ABC-fractional derivative in simulation generates a chaotic system for a relatively short period of time. The ABC-fractional derivative, in the context of Caputo, is an effective mathematical method for modeling progressively more critical difficulties than the power and exponential kernels. Due to their vast repercussions, these formulations are generally known for their intrinsic non-orientation, which results in fractional differential equations (DEs) without artificial anomalies, as in the context of the Riemann-Liouville and Caputo derivatives [19]. We have also observed a growing interest in mathematical techniques among these operators. However, as can be seen in [20], estimating these derivatives numerically leads to a number of computational problems. Since they have piqued the attention of several researchers who investigate their behavior in terms of solvability, uniqueness, and the stability of their solutions, particularly nonlinearity, these complicated issues have been researched in the literature [21]. Nonlinear processes do not always have realistic analytical solutions since it might be challenging to find the appropriate solutions by putting them into ordinary or fractional DEs.

According to the criteria of solvability, distinctiveness, and stabilization of the solutions of mathematical models, particularly nonlinear DEs, this has piqued the curiosity of numerous scholars who have investigated them in literature and classified them as nonlinear or linear [22,23]. Nonlinear processes do not necessarily have precise approximate solutions because it is difficult to find results by putting them in the context of ordinary or fractional DEs [24–26]. Due to this challenge, scientists have concentrated on creating a number of numerical techniques to discover an approximation of the outcome. Numerous methods are used to find the analytical solutions for integral equations and nonlinear coupled fractional DEs [27–29]. Analytical solutions of the coupled fractional DEs have been derived by taking into account the Homotopy perturbation method (HPM) [30], Adomian decomposition method [31], new iterative transform method [32], Lie symmetry analysis [33], reproducing kernel Hilbert space method [34], spectral collocation method [35], wavelet transform method [36], Chebyshev spectral collocation method [37] and henceforth.

In addition to J. B. Fourier's (1768–1830) dissertation "La Théorie Analytique de La chaleur" (1822), documented in [38], P. S. Laplace's (1749–1827) research on mathematical statistics in the 1780s is credited with helping to establish the integral transform applied in academia to find conclusions. The complex dynamical issues could not be solved by integral transformations such as Laplace, Sumudu, and so forth. For this reason, several mathematicians have explored new techniques to solve nonlinear fractional DEs. To make the technique of addressing partial and ordinary DEs in the context of spatial-temporal analysis easier. In 2016, Zafar [39,40] proposed a novel transform. This new transformation is a refinement of the Laplace and Aboodh transforms that are already in practice and can be used in a similar manner to identify the analytical solutions to the fractional SIR epidemic model [41].

However, the HPM's capacity to manage problems involving singularities, including those prevalent in science and technology, constitutes one of its main strengths. Scientists have started investigating the application of the HPM in conjunction with other transforms. A mathematical method called the homotopy perturbation-$\mathcal{ZZ}$ transform method (HP-$\mathcal{ZZ}$TM) can be utilized for transforming a dynamical problem into a linear equation, which will increase the system's solvability, precision and supremacy. Scientists have improved the effectiveness and precision of solving a variety of nonlinear challenges by employing the HPM and the $\mathcal{ZZ}$ transform. In general, it seems to have been demonstrated that the HPM with the $\mathcal{ZZ}$ transform is a robust and productive method for handling nonlinear challenges, with a wide range of feasible implementations in different domains [42–45].

Adopting the aforesaid propensity, we aim to investigate the attacking behavior of worms in WSN by employing the ABC fractional derivative operator in the frame of the GMLF. Several characterizations of the $\mathcal{ZZ}$ transform in terms of the ABC fractional derivative operator are provided, which is the main motivation of this work. To the best of our knowledge, the worms propagation in WSNs in the context of fractional operators is less of a consideration due to heavy virus attacks. In order to cope with this issue, we presented a new scheme for merging the worms propagation in WSNs in a fractional sense to get a better understanding. Also, a detailed description of worm propagation in WSNs can be accessed by employing statistical analysis such as the 0–1 test, the approximate entropy assessment, and the complexity of the system.

Taking into consideration the well-noted $\mathcal{ZZ}$ transform, we constructed a new algorithm by using HPM, which is known as homotopy perturbation $\mathcal{ZZ}$ transform method (HP-$\mathcal{ZZ}$TM). According to the five-cohort epidemic model and with the aid of HP-$\mathcal{ZZ}$T, we proposed analytical solutions for the process of worm dissemination in relation to time in WSNs. We presuppose that additional node sensors will be added and that cells will stop functioning as a result of malware attacks and software or hardware defects in the monitoring domain. It is assumed that every sensor node inside the sensor region is vulnerable to potential worm attacks. Because worms proliferate easily, they may invade a single detector component, which then eventually spreads to adjoining sensors by creating a contagious type of access points and fusion centers. The sensor nodes exhibit attack signs, such as a slowdown in the typical information communication rapidity, prior to ultimately becoming infected. These node classifications are placed in an accessible compartment in the form of an ABC fractional operator. Our proposed model can enhance the system's anti-virus performance and allow it to modify itself more easily for various types of viruses by adding an operational procedure to the WSN's sleep networks when reducing the fractional-order. Due to the lack of permanent immunization in the cyber world, nodes emerge briefly protective before becoming vulnerable to potential worm attacks when fractional-order reduces to 1. Several properties of the worms propagation in WSN are discussed, such as worm-free equilibrium, endemic state, basic reproduction number, and stability analysis. Further, modeling depictions indicate the system's behavior for various fractional-orders. A comprehensive review related to our outcomes explains the existence and uniqueness of the model. System parameters enhance the variability and trustworthiness of the sensor nodes for detecting malware. In a nutshell, this analytical technique will open new venues in the research of applied sciences and technological disciplines.

2. Preliminaries

Firstly, several key lemmas and an explanation of the ABC fractional-order derivative are given. Illustrations of time-dependent fractional-order WP in the WSNs model are then presented.

Definition 2.1. ([46]) Assuming that $p_1 \in (1,\infty)$ and $\mathfrak{O}_1$ correspond to open subsets of $\mathbb{R}$, the Sobolev space $\Omega^{p_1}(\mathfrak{O}_1)$ is given as follows:

$$\Omega^{p_1}(\mathfrak{O}_1) = \left\{\mathcal{G} \in \mathcal{L}^2(\mathfrak{O}_1) : D^{\wp}\mathcal{G} \in \mathcal{L}^2(\mathfrak{O}_1),\ \forall\ |\wp| \le p_1\right\}. \tag{2.1}$$

Definition 2.2. ([18]) Suppose that $\mathcal{G} \in H^1(0,1)$ and $0 < \wp \le 1$. The ABC fractional derivative of a mapping $\mathcal{G}$ can be defined as:

$${}^{ABC}D_{\zeta}^{\wp}\mathcal{G}(\zeta) = \frac{\Lambda(\wp)}{1-\wp}\int_0^{\zeta} E_{\wp}\left[-\frac{\wp}{(1-\wp)}(\zeta-\tau)^{\wp}\right]\mathcal{G}'(\tau)\,d\tau, \tag{2.2}$$

where $\mathcal{E}_{\wp}$ is the well-known Mittag-Leffler function of one parameter and $\Lambda(\wp) = 1-\wp+\frac{\wp}{\Gamma(\wp)}$ is a normalization function satisfying $\Lambda(0) = \Lambda(1) = 1$.

Definition 2.3. ([47]) The corresponding fractional integral operator of (2.2) can be addressed as:

$${}^{AB}\mathcal{I}_{\zeta}^{0}\mathcal{G}(\zeta) = \frac{1-\wp}{\Lambda(\wp)}\mathcal{G}(\zeta) + \frac{\wp}{\Lambda(\wp)\Gamma(\wp)}\int_0^{\zeta}\mathcal{G}(\tau)(\zeta-\tau)^{\wp-1}d\tau, \tag{2.3}$$

where Γ symbolizes well-known Gamma function is defined as $\Gamma(\sigma) = \int_0^{\infty}\zeta^{\sigma-1}e^{-\zeta}\,d\zeta$.

For more details on the characterization of the ABC fractional derivative, we refer the readers to [48].

Lemma 2.1. *([[49]]) **(Generalized mean value theorem)** Let $\mathcal{F}(\varkappa) \in C[\mathbf{c}_1,\mathbf{c}_2]$ and assume that ${}^{ABC}D_{\zeta}^{\wp}\mathcal{F}(\varkappa) \in C[\mathbf{c}_1,\mathbf{c}_2]$, where, $0 < \wp \le 1$. Then we have*

$$\mathcal{F}(\varkappa) = \mathcal{F}(\mathbf{c}_1) + \frac{1}{\Gamma(\wp)}\,{}^{ABC}D_{\zeta}^{\wp}\mathcal{F}()(\varkappa-\mathbf{c}_1)^{\wp},$$

when $0 \le \varphi \le \varkappa,\ \forall\ \varkappa \in [\mathbf{c}_1,\mathbf{c}_2]$.

Theorem 2.1. *([50]) For a function $\mathcal{G} \in H^1[\tau,\varrho]$, the following results hold:*

$$\|\,{}^{ABC}D_{\zeta}^{\wp}\mathcal{G}(\zeta)\| < \frac{\Lambda(\wp)}{1-\wp}\|c_1(\zeta)\|,\ \textit{where}\ \|c_1(\zeta)\| = max_{\tau\le\zeta\le\varrho}|c_1(\zeta)|.$$

Additionally, the derivatives of ABC satisfy the Lipschitz criterion [51]:

$$\|\,{}^{ABC}D_{\zeta}^{\wp}c_1(\zeta) - {}^{ABC}D_{\zeta}^{\wp}c_2(\zeta)\| < \omega\|c_1(\zeta)-c_2(\zeta)\|. \tag{2.4}$$

2.1. New features of the $\mathcal{ZZ}$ transform

We present some fundamental ideas and characteristics of the $\mathcal{ZZ}$ transform, which is mainly due to [52].
Define the set

$$\mathcal{A}_1 = \left\{\mathcal{G}(\zeta) : \exists\ \mathcal{M} > 0,\ \varsigma > 0,\ |\mathcal{G}(\zeta)| \le \mathcal{M}e^{\varsigma\zeta},\ if\ \zeta \ge 0\right\}. \tag{2.5}$$

In the same way, we will assume that $\mathcal{G}(\zeta)$ is an integrated function defined on set $\mathcal{A}$.

Definition 2.4. ([52]) Assume that there is a function $\mathcal{G}(\zeta)$ defined for all values of $\zeta \ge 0$. The $\mathcal{ZZ}$ transform of $\mathcal{G}(\zeta)$ is the function $\mathcal{F}[\varpi,\varphi]$ defined by

$$\mathcal{Z}\left[\mathcal{G}(\zeta)\right] = \mathcal{F}(\varpi,\varphi) = \varphi\int_0^{\infty}\mathcal{G}(\varpi\zeta)\,e^{-\varphi\zeta}d\zeta. \tag{2.6}$$

The integral transform (2.6) exists for all $\frac{\varphi}{\varpi} > \varsigma$.

Table 1
Description of transform.

$\mathcal{G}(\zeta)$	$\mathcal{Z}[\mathcal{G}(\zeta)]$
1	1
ζ	$\frac{\varpi}{\varphi}$
$\zeta^{\mathfrak{n}}$	$n!\ \frac{\varpi^{\mathfrak{n}}}{\varphi^{\mathfrak{n}}}$, $\mathfrak{n}=0,1,2,...$
$\zeta^{\wp}$	$\Gamma(\wp+1)\ \frac{\varpi^{\wp}}{\varphi^{\wp}}$, $\wp\geq 0$

Theorem 2.2. *The $\wp^{th}$ derivative of $\mathcal{G}(\zeta)$ and $\mathcal{ZZ}$ transform can be obtained by*

$$\mathcal{Z}\left[\mathcal{G}^{\wp}(\zeta)\right](\varphi,\varpi)=\left(\frac{\varphi}{\varpi}\right)^{\wp}\mathcal{Z}\left[\mathcal{G}(\zeta)\right]-\sum_{\ell=0}^{\mathfrak{n}-1}\left(\frac{\varphi}{\varpi}\right)^{\wp-\ell}\mathcal{G}^{(\ell)}(0),\quad \frac{\varphi}{\varpi}>0,\forall\ \wp\in\mathbb{N}. \tag{2.7}$$

Theorem 2.3. *The $\mathcal{ZZ}$ transformation in the combination of functions $\mathcal{G}(\zeta)$ and $\mathcal{Q}(\zeta)$ can be presented as*

$$\mathcal{Z}\left[\mathcal{G}.\mathcal{Q}\right]\ =\ \mathcal{Z}[\mathcal{G}]*\mathcal{Z}[\mathcal{Q}].$$

Therefore, we have

$$\mathcal{Z}^{-1}\left[\mathcal{G}.\mathcal{Q}\right]\ =\ \mathcal{Z}^{-1}[\mathcal{G}]*\mathcal{Z}^{-1}[\mathcal{Q}].$$

Proof. It suffices to note that

$$\left[\mathcal{G}.\mathcal{Q}\right]=\int_0^{\infty}\mathcal{G}(\varkappa)\mathcal{Q}(\zeta-\varkappa)\ d\varkappa.$$

Using the Leibnitz theorem and the $\mathcal{ZZ}$ transformation, we have

$$\mathcal{Z}[\mathcal{G}*\mathcal{Q}]=\mathcal{Z}\left[\int_0^{\infty}\mathcal{G}(\varkappa)\mathcal{Q}(\zeta-\varkappa)\ d\varkappa\right]=\varphi\int_0^{\infty}\left[\int_0^{\infty}\mathcal{G}(\varkappa)\mathcal{Q}(\zeta-\varkappa)d\varkappa\right]e_1^{-\varphi\zeta}\ d\varkappa.$$

By putting $\mathcal{Y}=\ \zeta-\varkappa$, then we have

$$\begin{aligned}\mathcal{Z}\left[\mathcal{G}*\mathcal{Q}\right]\ &=\varphi\int_0^{\infty}\mathcal{G}(\varkappa)e_1^{-\varphi\varkappa}\left\{\int_0^{\infty}\mathcal{Q}(\tau)d\tau\right\}d\varkappa\\&=\varphi\int_0^{\infty}\mathcal{G}(\varkappa)e_1^{-\varphi\varkappa}d\varkappa.\mathcal{Z}[\mathcal{Q}]\\&=\mathcal{Z}[\mathcal{G}].\mathcal{Z}[\mathcal{Q}].\end{aligned}$$

Also, the reverse transformation's combination is

$$\mathcal{Z}\left[\mathcal{Z}^{-1}(\mathcal{G})*\mathcal{Z}^{-1}(\mathcal{Q})\right]=\mathcal{G}.\mathcal{Q}.$$

It follows that

$$\mathcal{Z}^{-1}[\mathcal{G}.\mathcal{Q}]=\mathcal{Z}^{-1}(\mathcal{G})*\mathcal{Z}^{-1}(\mathcal{Q}).\quad\square$$

2.2. Multiple elementary function by $\mathcal{ZZ}$ transformed

Now, we will show how some basic functions are transformed using the $\mathcal{ZZ}$ transform presented in Table 1, then we have:

Lemma 2.2. *Let $0<\mathfrak{n}<1$ and $\varsigma\in\mathcal{R}$ such that $\frac{\varphi}{\varpi}<|\ \varsigma\ |^{\frac{1}{\mathfrak{n}}}$, then we have*

$$\mathcal{Z}[\zeta^{\wp-1}]E^{\sigma}_{\mathfrak{n},\wp}\left(\varsigma,\zeta^{\mathfrak{n}}\right)(\varphi,\varpi)=\left(\frac{\varpi}{\varphi}\right)^{\rho_1}.\left(1-\varsigma\left(\frac{\varpi}{\varphi}^{\mathfrak{n}}\right)\right)^{-\sigma},\quad\frac{\varphi}{\varpi}>0.$$

Proof. Assume that

$$\begin{aligned}
\mathcal{Z}[\zeta^{\wp-1}]E^{\sigma}_{\mathrm{n},\wp}\left(\varsigma,\zeta^{\mathrm{n}}\right)(\varphi,\varpi) &= \frac{\varphi}{\varpi}\int_0^{\infty}\zeta^{\wp-1}E^{\sigma}_{\mathrm{n},\wp}\left(\varsigma.\zeta^{\mathrm{n}}\right)e_1^{\frac{-\varphi}{\varpi}}d\zeta\\
&= \frac{\varphi}{\varpi}\int_0^{\infty}\zeta^{\wp-1}\sum_{\ell=0}^{\infty}\frac{\sigma\ell}{\Gamma(\mathrm{n}\ell+\wp)}.\frac{(\varsigma\zeta^{\mathrm{n}})^{\ell}}{k!}\,e_1^{\frac{-\varphi}{\varpi}}d\zeta\\
&= \sum_{\ell=0}^{\infty}\frac{\sigma\ell}{\Gamma(\mathrm{n}\ell+\wp)}.\left(\frac{\varsigma^{\ell}}{\ell!}\right)\left(\frac{\varphi}{\varpi}\right)\int_0^{\infty}\zeta^{\mathrm{n}\ell+\wp-1}\,e_1^{-\frac{\varphi}{\varpi}}d\zeta\\
&= \sum_{\ell=0}^{\infty}\frac{\sigma\ell}{\Gamma(\mathrm{n}\ell+\wp)}.\left(\frac{\varsigma^{\ell}}{\ell!}\right)\left(\frac{\varphi}{\varpi}\right)\mathcal{Z}\left[\zeta^{\mathrm{n}\ell+\wp-1}\right]\\
&= \sum_{\ell=0}^{\infty}\frac{\sigma\ell}{\Gamma(\mathrm{n}\ell+\wp)}.\left(\frac{\varsigma^{\ell}}{\ell!}\right)\left(\frac{\varphi}{\varpi}\right)(\Gamma(\mathrm{n}\ell+\wp)\left(\frac{\varpi}{\varphi}\right)^{\mathrm{n}\ell+\sigma}\\
&= \left(\frac{\varpi}{\varphi}\right)^{\wp}.\sum_{\ell=0}^{\infty}\frac{\sigma\ell}{\ell!}\left[\varsigma\left(\frac{\varpi}{\varphi}\right)^{\mathrm{n}}\right]^{\ell}.
\end{aligned}$$

According to $\frac{\varphi}{\varpi}<|\varsigma|^{\frac{1}{\mathrm{n}}}$ leads us

$$\mathcal{Z}\left[\zeta^{\wp-1}E^{\sigma}_{\mathrm{n},\wp}(\varsigma,\zeta^{\mathrm{n}})(\varphi,\varpi)\right]=\left(\frac{\varpi}{\varphi}\right)^{\wp}\left(1-\varsigma\left(\frac{\varpi}{\varphi}\right)^{\mathrm{n}}\right)^{-\sigma}. \quad \square$$

Corollary 2.1. *Under the hypothesis of Lemma 2.2, we can calculate the $\mathcal{ZZ}$ transform of the function $E_{\mathrm{n}}(\varsigma,\zeta^{\mathrm{n}})$, then we have*

$$\mathcal{Z}\left[E_{\mathrm{n}}(\varsigma,\zeta^{\mathrm{n}})\right](\varphi,\varpi)=\left(\frac{\varpi}{\varphi}\right)\left(\frac{(\frac{\varphi}{\varpi})^{\mathrm{n}}}{(\frac{\varphi}{\varpi})^{\mathrm{n}}-\varsigma}\right).$$

Thus, the $\mathcal{ZZ}$ transform of $\zeta^{\wp-1}E_{\mathrm{n}}(\varsigma,\zeta^{\mathrm{n}})$ can be written as:

$$\mathcal{Z}\left[\zeta^{\wp-1}\;E_{\mathrm{n}}\left(\varsigma,\zeta^{\mathrm{n}}\right)\right](\varphi,\varpi)=\left(\frac{(\frac{\varphi}{\varpi})^{\mathrm{n}-\wp}}{(\frac{\varphi}{\varpi})^{\mathrm{n}}-\varsigma}\right).$$

Theorem 2.4. *The $\mathcal{ZZ}$ transform of the ABC fractional derivative ${}^{ABC}D^{\wp}_{\zeta}$ is defined as:*

$$\mathcal{Z}\left[{}^{ABC}D^{\wp}_{\zeta}\mathcal{G}(\zeta)\right](\varpi,\varphi)=\frac{\Lambda(\wp)}{1-\wp}*\left(\frac{\mathcal{Z}[\mathcal{G}(\zeta)](\frac{\varphi}{\varpi})^{\wp}-(\frac{\varphi}{\varpi})^{\wp-1}\mathcal{G}(0)}{(\frac{\varphi}{\varpi})^{\wp}+\frac{\wp}{1-\wp}}\right).$$

Proof. It suffices to note that

$$\int_0^{\zeta}\mathcal{G}'(\varkappa)E_{\wp}\left[\frac{\wp}{\wp-1}(\zeta-\varkappa)^{\wp}\right]d\varkappa=\mathcal{G}'(\zeta).E_{\wp}\left[\frac{\wp}{\wp-1}\zeta^{\wp}\right],$$

then one has

$$\begin{aligned}
\mathcal{Z}\left[{}^{ABC}D^{\wp}_{\zeta}\mathcal{G}(\zeta)\right](\varpi,\varphi) &= \mathcal{Z}\left[\frac{\Lambda(\wp)}{1-\wp}\int_0^{\zeta}\mathcal{G}'(\varkappa)E_{\wp}\Big(\frac{\wp}{\wp-1}(\zeta-\varkappa)^{\wp}d\varkappa\Big)\right]\\
&= \frac{\Lambda(\wp)}{1-\wp}\;\mathcal{Z}\left[\mathcal{G}'(\zeta)E_{\wp}\Big(\frac{\wp}{\wp-1}\zeta^{\wp}\Big)\right]\\
&= \frac{\Lambda(\wp)}{1-\wp}\;\mathcal{Z}[\mathcal{G}'(\zeta)]\mathcal{Z}\left[E_{\wp}\Big(\frac{\wp}{\wp-1}\zeta^{\wp}\Big)\right].
\end{aligned}$$

Utilizing (2.7) and the outcome from Corollary 2.1, we have

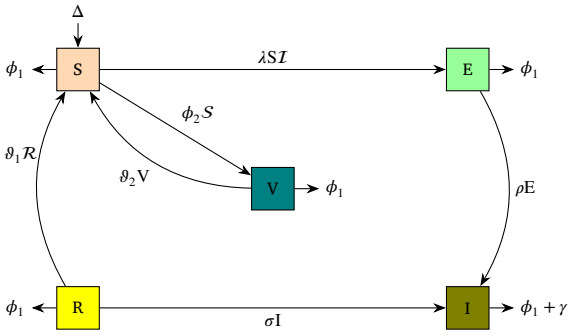

Fig. 2. Flow diagram for depicting the WP model in WSN (3.1).

$$\mathcal{Z}\left[{}^{ABC}D_{\zeta}^{\wp}\mathcal{G}(\zeta)\right](\varpi,\varphi) = \frac{\Lambda(\wp)}{1-\wp}\left[\frac{\varphi}{\varpi}\mathcal{Z}[\mathcal{G}(\zeta)] - \mathcal{G}(0)\right]\left(\frac{\varpi}{\varphi}\right)\left\{\frac{(\frac{\varphi}{\varpi})^{\wp}}{(\frac{\varphi}{\varpi})^{\wp} - \frac{\wp}{\wp-1}}\right\}$$

$$= \frac{\Lambda(\wp)}{1-\wp}\left\{\frac{\mathcal{Z}[\mathcal{G}(\zeta)](\frac{\varphi}{\varpi})^{\wp} - (\frac{\varphi}{\varpi})^{\wp-1}\mathcal{G}(0)}{(\frac{\varphi}{\varpi})^{\wp} + \frac{\wp}{1-\wp}}\right\}. \quad \square$$

3. Configuration of WP model in WSNs

Let us explain the $\mathcal{S}(\zeta)$, $\mathcal{E}(\zeta)$, $\mathcal{I}(\zeta)$, $\mathcal{R}(\zeta)$ and $\mathcal{V}(\zeta)$ of nodes that are sensitive, revealed, infected, retrieved and vaccinate at time ζ. Taking $\mathcal{N}(\zeta) = \mathcal{S}(\zeta) + \mathcal{E}(\zeta) + \mathcal{I}(\zeta) + \mathcal{R}(\zeta) + \mathcal{V}(\zeta),\ \forall\ \zeta > 0$.
The system of DEs, represented by Fig. 2, which describes the rate of change of multiple categories and according to our assumptions, is presented as follows:

$$\begin{cases} \dot{\mathcal{S}}(\zeta) = \Delta - \lambda\mathcal{S}(\zeta)\mathcal{I}(\zeta) - (\phi_1 + \phi_2)\mathcal{S}(\zeta) + \vartheta_1\mathcal{R}(\zeta) + \vartheta_2\mathcal{V}(\zeta), \\ \dot{\mathcal{E}}(\zeta) = \lambda\mathcal{S}(\zeta)\mathcal{I}(\zeta) - (\phi_1 + \rho)\mathcal{E}(\zeta), \\ \dot{\mathcal{I}}(\zeta) = \rho\mathcal{E}(\zeta) - (\phi_1 + \gamma + \sigma)\mathcal{I}(\zeta), \\ \dot{\mathcal{R}}(\zeta) = \sigma\mathcal{I}(\zeta) - (\phi_1 + \vartheta_1)\mathcal{R}(\zeta), \\ \dot{\mathcal{V}}(\zeta) = \phi_2\mathcal{S}(\zeta) - (\phi_1 + \vartheta_2)\mathcal{V}(\zeta), \end{cases} \tag{3.1}$$

where Δ represents the inclusion of new sensor nodes to the population, $\frac{1}{\vartheta_1}$ and $\frac{1}{\vartheta_2}$ represent the periods of exception for immediately recovered and given vaccinations sensitive nodes, respectively, ϕ_1 is the crash rate of the sensor nodes due to hardware or software, γ is the damaged rate due to invasion of worms and the infection contact rate is represented by λ, where ρ is the E-compartment to I-compartment transfer rate, σ represents a recapture rate, ϑ_1 is the rate of transmission from $\mathcal{V}$-compartment to $\mathcal{S}$-compartment and ϕ_2 is the vaccinating rate coefficient for the sensitive nodes.

3.1. Fractional-order WP model in WSNs

In what follows, one of these exceptional systems has been identified. The authors categorized the whole community into five groups. These include WP in WSNs that is susceptible class $\mathcal{S}$, exposed class $\mathcal{E}$, infected class $\mathcal{I}$, recovered class $\mathcal{R}$, and vaccinated class $\mathcal{V}$, respectively. The examined approach is translated into a fractional version. Order $\wp$ $(0 < \wp \leq 1)$ and the fractional operator are added to the ABC fractional version, resulting in the following:

$$\begin{cases} {}^{ABC}D_{\zeta}^{\wp}\mathcal{S}(\zeta) = \Delta - \lambda\mathcal{S}(\zeta)\mathcal{I}(\zeta) - (\phi_1 + \phi_2)\mathcal{S}(\zeta) + \vartheta_1\mathcal{R}(\zeta) + \vartheta_2\mathcal{V}(\zeta), \\ {}^{ABC}D_{\zeta}^{\wp}\mathcal{E}(\zeta) = \lambda\mathcal{S}(\zeta)\mathcal{I}(\zeta) - (\phi_1 + \rho)\mathcal{E}(\zeta), \\ {}^{ABC}D_{\zeta}^{\wp}\mathcal{I}(\zeta) = \rho\mathcal{E}(\zeta) - (\phi_1 + \gamma + \sigma)\mathcal{I}(\zeta), \\ {}^{ABC}D_{\zeta}^{\wp}\mathcal{R}(\zeta) = \sigma\mathcal{I}(\zeta) - (\phi_1 + \vartheta_1)\mathcal{R}(\zeta), \\ {}^{ABC}D_{\zeta}^{\wp}\mathcal{V}(\zeta) = \phi_2\mathcal{S}(\zeta) - (\phi_1 + \vartheta_2)\mathcal{V}(\zeta), \end{cases} \tag{3.2}$$

with the initial conditions (ICs):

$$\mathcal{S}(0) = \mathcal{W}_1 \geq 0, \quad \mathcal{E}(0) = \mathcal{W}_2 \geq 0, \quad \mathcal{I}(0) = \mathcal{W}_3 \geq 0, \quad \mathcal{R}(0) = \mathcal{W}_4 \geq 0, \quad \mathcal{V}(0) = \mathcal{W}_5 \geq 0, \tag{3.3}$$

where $0 \leq \zeta \leq \mathcal{T} < \infty$ and ${}^{ABC}D_{\zeta}^{\wp}$ indicates the ABC fractional derivative of order $0 < \wp \leq 1$.

We outlined the fundamental characteristics of framework (3.2) in order to establish the mathematical system's well-posedness and biological viability.

3.2. Positive invariant and boundedness

By applying Lemma 2.1 to prove the system's positivity, we have

$$\begin{cases} {}^{ABC}\mathcal{D}_{\zeta}^{\wp}\mathcal{S}(\zeta)|_{S=0} = \Delta \geq 0, \\ {}^{ABC}\mathcal{D}_{\zeta}^{\wp}\mathcal{E}(\zeta)|_{\mathcal{E}=0} = 0 \geq 0, \\ {}^{ABC}\mathcal{D}_{\zeta}^{\wp}\mathcal{I}(\zeta)|_{\mathcal{I}=0} = \rho\mathcal{E}(\zeta) \geq 0, \\ {}^{ABC}\mathcal{D}_{\zeta}^{\wp}\mathcal{R}(\zeta)|_{\mathcal{R}=0} = \sigma\mathcal{I}(\zeta) \geq 0, \\ {}^{ABC}\mathcal{D}_{\zeta}^{\wp}\mathcal{V}(\zeta)|_{\mathcal{V}=0} = \phi_2\mathcal{S}(\zeta) \geq 0. \end{cases} \tag{3.4}$$

Since (3.4) implies that each of the solutions of WP model (3.2) is positive, they stay in $\mathbb{R}_5^+$. Ultimately, considering that all of the parameters are positive, we proceed by adding up all of the model's equations in order to prove the boundedness of the solutions of the fractional model (3.2). This yields

$${}^{ABC}\mathcal{D}_{\zeta}^{\wp}\mathcal{N}(\zeta) = \Delta - \phi_1\mathcal{N}(\zeta) - \gamma\mathcal{I}.$$

It follows that

$${}^{ABC}\mathcal{D}_{\zeta}^{\wp}\mathcal{N}(\zeta) \leq \Delta - \phi_1\mathcal{N}(\zeta). \tag{3.5}$$

In this case, set $\mho_1$ defined in (3.6) is positively invariant for the model (3.2). Therefore, the WP model (3.2)'s epidemiologically feasible zone is provided by

$$\mho_1 =: \left\{(\mathcal{S},\mathcal{E},\mathcal{I},\mathcal{R},\mathcal{V}) \in \mathbb{R}_5^+ : 0 \leq \mathcal{S}+\mathcal{E}+\mathcal{I}+\mathcal{R}+\mathcal{V} \leq \mathcal{N} \leq \frac{\Delta}{\phi_1}\right\}. \tag{3.6}$$

Furthermore, the existence and uniqueness solution of the worms propagation model (3.2) have been established, the only thing left to demonstrate is the positively invariant nature of the set defined in (3.6). Applying the Laplace transform to (3.5), then we have

$$\mathcal{L}\left({}^{ABC}\mathcal{D}_{\zeta}^{\wp}\mathcal{N}(\zeta)) + \phi_1\mathcal{N}(\zeta)\right) \leq \mathcal{L}(\Delta).$$

It can be expressed as

$$\begin{aligned} \mathcal{L}(\mathcal{N})\left((1-\Xi)\mathbf{s}^{\wp} - \frac{\Xi\wp}{(1-\wp)}\right) - \mathbf{s}^{\wp-1}\mathcal{N}(0) &\leq \frac{1-\wp}{\Lambda(\wp)}\left(\mathbf{s}^{\wp} + \frac{\wp}{1-\wp}\right)\frac{\Delta}{\mathbf{s}} \\ &\leq \left(1 - \frac{\Xi\wp}{(1-\Xi)(1-\wp)}\mathbf{s}^{-\wp}\right)^{-1}\left[\frac{1-\wp}{(1-\wp)\Phi(\wp)}\left(1 + \frac{\wp}{1-\wp}\mathbf{s}^{-\wp}\right)\frac{\Delta}{\mathbf{s}}\right. \\ &\quad \left. + \mathcal{N}(0)\frac{1}{(1-\Xi)\mathbf{s}}\right]. \end{aligned}$$

Choosing

$$\Xi = \frac{-\phi_1(1-\wp)}{\Lambda(\wp)}.$$

After implementing the inverse Laplace transform according to work [53], the solution is presented as

$$\begin{aligned} \mathcal{N}(\zeta) = \frac{\Delta}{\phi_1} - \frac{\Delta}{\phi_1(1-\Xi)}\frac{d}{d(\zeta)}\int_0^{\zeta}\mathcal{E}_{\wp}\left(\frac{\Xi\wp}{(1-\Xi)(1-\wp)}(\zeta-\varkappa)^{\wp}d\varkappa\right) \\ + \frac{1}{1-\Xi}\mathcal{E}_{\wp}\left(\frac{\Xi\wp}{(1-\Xi)(1-\wp)}\zeta\right)\mathcal{N}(0), \end{aligned}$$

where the Mittag-Leffler function is indicated by $\mathcal{E}_{\rho,\Phi}$. It is worthnoting that the Mittag-Leffler function exhibits asymptotic behavior such as

$$\mathcal{E}_{\rho,\Phi}(z_1) \approx \sum_{\Xi=1}^{w_1} t^{-\Xi}/\Gamma(\Phi - \rho\Xi) + \mathcal{O}\left(|\zeta|^{-1-w_1}\right), |\zeta| \to \infty, \frac{\wp\pi}{2} < |arg(\zeta)| \leq \pi,$$

it is not difficult to observe that $\mathcal{N}(\zeta) \to \frac{\Delta}{\phi_1}$ as $\zeta \to \infty$. Hence, (3.6) is the biologically feasible region of model (3.2).

3.3. Worm-free equilibrium

For worm-free equilibrium, equating the left-hand side of (3.4) to zero, we have

$$\begin{cases} 0 = \Delta - \lambda S(\zeta)\mathcal{I}(\zeta) - (\phi_1 + \phi_2)S(\zeta) + \vartheta_1\mathcal{R}(\zeta) + \vartheta_2\mathcal{V}(\zeta), \\ 0 = \lambda S(\zeta)\mathcal{I}(\zeta) - (\phi_1 + \rho)\mathcal{E}(\zeta), \\ 0 = \rho\mathcal{E}(\zeta) - (\phi_1 + \gamma + \sigma)\mathcal{I}(\zeta), \\ 0 = \sigma\mathcal{I}(\zeta) - (\phi_1 + \vartheta_1)\mathcal{R}(\zeta), \\ 0 = \phi_2 S(\zeta) - (\phi_1 + \vartheta_2)\mathcal{V}(\zeta). \end{cases} \tag{3.7}$$

After simple computations, we obtain the equilibrium points as follows:

$$\mathcal{P} = \left(\frac{\Delta(\phi_1 + \vartheta_2)}{\phi_1(\phi_1 + \vartheta_2 + \phi_2)}, 0, 0, 0, \frac{\phi_2\Delta}{(\phi_1 + \vartheta_1)(\phi_1 + \phi_2) - \phi_2\vartheta_2} \right).$$

3.4. Endemic equilibrium point (EEP)

For endemic equilibrium point, when the population's virus rate continues to persist. In the absence of viruses throughout the population, the worm-free equilibrium for the WP model is determined by

$$\begin{aligned} \mathcal{S}^* &= \frac{(\phi_1 + \rho)(\phi_1 + \gamma + \sigma)}{\rho\lambda}, \\ \mathcal{E}^* &= \frac{(\phi_1 + \gamma + \sigma)(\phi_1 + \vartheta_1)}{\{\sigma\rho\vartheta_1 - (\phi_1 + \vartheta_1)(\phi_1 + \rho)(\phi_1 + \gamma + \sigma)\}\rho} \left[\frac{(\phi_1 + \rho)(\phi_1 + \gamma + \sigma)}{\lambda} . \frac{(\phi_1 + \phi_2)(\phi_1 + \vartheta_2) - \vartheta_2\phi_2}{\phi_1 + \vartheta_2} - \rho\Delta \right], \\ \mathcal{I}^* &= \frac{(\phi_1 + \vartheta_1)}{\sigma\rho\vartheta_1 - (\phi_1 + \vartheta_1)(\phi_1 + \rho)(\phi_1 + \gamma + \sigma)} \left[\frac{(\phi_1 + \rho)(\phi_1 + \gamma + \sigma)}{\lambda} . \frac{(\phi_1 + \phi_2)(\phi_1 + \vartheta_2) - \vartheta_2\phi_2}{\phi_1 + \vartheta_2} - \rho\Delta \right], \\ \mathcal{R}^* &= \frac{\sigma}{\left(\sigma\rho\vartheta_1 - (\phi_1 + \vartheta_1)(\phi_1 + \rho)(\phi_1 + \gamma + \sigma)\right)} \left[\frac{(\phi_1 + \rho)(\phi_1 + \gamma + \sigma)}{\lambda} . \frac{(\phi_1 + \phi_2)(\phi_1 + \vartheta_2) - \vartheta_2\phi_2}{\phi_1 + \vartheta_2} - \rho\Delta \right], \\ \mathcal{V}^* &= \frac{\phi_2(\phi_1 + \rho)(\phi_1 + \gamma + \sigma)}{(\phi_1 + \vartheta_2)\rho\lambda}. \end{aligned}$$

3.5. The basic reproduction number R_0

In this case, the $\mathcal{E}$ and $\mathcal{I}$ compartments are both compartments for virus.
Let $\mathcal{X} = (\mathcal{E}, \mathcal{I})$, set $\mathcal{F} = \begin{Bmatrix} \lambda S\mathcal{I} \\ 0 \end{Bmatrix}$ and $\mathcal{V} = \begin{Bmatrix} (\phi_1 + \rho)\mathcal{E} \\ \rho\mathcal{E} - (\phi_1 + \gamma + \sigma)\mathcal{I} \end{Bmatrix}$.

Thus, we consider that $\mathcal{X} = (\mathcal{E}, \mathcal{I}) = (\varkappa, x_2)$,

$$\frac{d\varkappa}{d\zeta} = \mathcal{F}(\varkappa, \tau) - \mathcal{V}(\varkappa, \tau) = \begin{Bmatrix} \lambda S x_2 \\ 0 \end{Bmatrix} - \begin{Bmatrix} (\phi_1 + \rho)\varkappa \\ \rho_1\varkappa - (\phi_1 + \gamma + \sigma)x_2 \end{Bmatrix}.$$

$$\mathcal{F} = \begin{bmatrix} \frac{\partial\phi_1}{\partial\varkappa} & \frac{\partial\phi_1}{\partial x_2} \\ \frac{\partial\mathcal{F}_2}{\partial\varkappa} & \frac{\partial\mathcal{F}_2}{\partial x_2} \end{bmatrix}_{\varkappa=0, x_2=0, S=\mathcal{N}} = \begin{bmatrix} 0 & \lambda \\ 0 & 0 \end{bmatrix}.$$

$$\mathcal{V} = \begin{bmatrix} \frac{\partial\mathcal{V}_1}{\partial\varkappa} & \frac{\partial\mathcal{V}_1}{\partial x_2} \\ \frac{\partial\mathcal{V}_2}{\partial\varkappa} & \frac{\partial\mathcal{V}_2}{\partial x_2} \end{bmatrix}_{\varkappa=0, x_2=0, S=\mathcal{N}} = \begin{bmatrix} \phi_1 + \rho & 0 \\ -\rho & (\phi_1 + \gamma + \sigma) \end{bmatrix}.$$

$\mathcal{V}$ and $\mathcal{F}$ can be calculated to get the fundamental reproduction number; these values can be obtained as

$$\mathcal{V} = \begin{bmatrix} \phi_1 + \rho & 0 \\ -\rho & \phi_1 + \gamma + \sigma \end{bmatrix},$$

$$\mathcal{F} = \begin{bmatrix} 0 & \lambda \\ 0 & 0 \end{bmatrix}.$$

The next generation matrix is

$$\mathcal{FV}^{-1} = \begin{bmatrix} \frac{\rho\lambda}{(\phi_1+\lambda)(\phi_1+\gamma+\sigma)} & \frac{\lambda}{(\phi_1+\gamma+\sigma)} \\ 0 & 0 \end{bmatrix}.$$

The entries $\frac{\rho\lambda}{(\phi_1+\lambda)(\phi_1+\gamma+\sigma)}$ *and* $\frac{\lambda}{(\phi_1+\gamma+\sigma)}$ are the expected number of secondary infections produced in the compartment by an individual initially in the compartment. $\mathcal{I}$ over the course of its infection and $\mathcal{E}$ infected individual originally in compartment $\mathcal{E}$.

As the dominant eigenvalue of $\mathcal{FV}^{-1}$, the basic reproduction number is expressed in the following way: i.e.,

$$\mathcal{R}_0 = \frac{\rho\lambda}{(\phi_1+\rho)(\phi_1+\gamma+\sigma)}.$$

3.6. Worm-free equilibrium stability

The Jacobin matrix in worm-free equilibrium point $\mathcal{P}$, then we have

$$\mathcal{J}_{\mathcal{P}} = \begin{bmatrix} -(\phi_1+\phi_2) & 0 & -\lambda\Delta(\phi_1+\vartheta_2) & \vartheta_1 & \vartheta_2 \\ 0 & -(\phi_1+\phi_2) & -\lambda\Delta(\phi_1+\vartheta_2) & 0 & 0 \\ 0 & 0 & -(\phi_1+\gamma+\sigma) & 0 & 0 \\ 0 & 0 & \sigma & -(\phi_1+\vartheta_1) & 0 \\ \phi_2 & 0 & 0 & 0 & -(\phi_1+\vartheta_2) \end{bmatrix}. \tag{3.8}$$

Eigenvalues of (3.8) are: $\chi = -(\phi_1+\phi_2), -(\phi_1+\rho), -(\phi_1+\gamma+\sigma), -(\phi_1+\vartheta_1), -(\phi_1+\vartheta_2)$ which are all non-positive, meaning that at the worm free equilibrium point $\mathcal{P}$, the system is locally asymptotically stable.

Lemma 3.1. *The worm-free equilibrium $\mathcal{P}$ is asymptotically stable locally if $\mathcal{R}_0 < 1$. $\mathcal{P}$ is stable if $\mathcal{R}_0 = 1$, and unstable if $\mathcal{R}_0 > 1$. Say that $\mathcal{Q}_\infty = \lim_{\zeta\to\infty} inf_{0\geq\zeta}\mathcal{Q}(\varpi)$, $\mathcal{Q}^\infty = \lim_{\zeta\to\infty}\ sup_{0\geq\zeta}\ \mathcal{Q}(\varpi)$.*

Lemma 3.2. *Suppose $\mathcal{Q} : [0,\infty] \to \mathcal{R}$ is a bounded, real-valued function that contains a bounded second derivative and is two times differentiable. If $\mathcal{Q}(t_k)$ converges to $\mathcal{Q}^\infty$ or $\mathcal{Q}_\infty$, let $\Xi \to \infty$.*
Then, we have

$$\lim_{\zeta\to\infty} \mathcal{Q}'(\zeta_\Xi) = 0$$

Theorem 3.1. *The worm-free equilibrium $\mathcal{P}$ is globally asymptotically stable if $\mathcal{R}_0 < 1$.*

Proof. From worm free equation

$$\frac{d\mathcal{S}}{d\zeta} \leq \Delta - \frac{\phi_1(\phi_1+\vartheta_2+\phi_2)}{\phi_1+\vartheta_2}\mathcal{S}.$$

A solution of the equation $\frac{d\mathcal{X}}{d\zeta} \leq \Delta - \frac{\phi_1(\phi_1+\vartheta_2+\phi_2)}{\phi_1+\vartheta_2}\mathcal{X}$ is solution of $\mathcal{S}(\zeta)$.
Since $\mathcal{X} \to \frac{(\phi_1+\vartheta_2)\Delta}{(\phi_1+\vartheta_2+\phi_2)\phi_1}$ as $\zeta\to\infty$, then for a given $\gamma > 0$, then exists t_0 such that

$$\mathcal{S}(\zeta) \leq \mathcal{X}(\zeta) \leq \frac{(\phi_1+\vartheta_2)\Delta}{(\phi_1+\vartheta_2+\phi_2)\phi_1} + \mathcal{E}\ \forall\ \zeta \geq \zeta_0.$$

Thus, we have

$$\mathcal{S}^\infty \leq \mathcal{X}(\zeta) \leq \frac{(\phi_1+\vartheta_2)\Delta}{(\phi_1+\vartheta_2+\phi_2)\phi_1} + \mathcal{E} \tag{3.9}$$

Let $\mathcal{E}\to 0$, *then* $\mathcal{S}^\infty \leq \frac{(\phi_1+\vartheta_2)\Delta}{(\phi_1+\vartheta_2+\phi_2)\phi_1}$. Now, worms propagation system (3.2) reduces to (3.8) as

$$\frac{d\mathcal{E}}{d\zeta} = \lambda\mathcal{I}\ \frac{(\phi_1+\vartheta_2)\Delta}{(\phi_1+\vartheta_2+\phi_2)\phi_1} - (\phi_1+\rho)\mathcal{E}$$

Now, considering (3.9) with worms propagation model (3.2), we have

$$\begin{bmatrix} \mathcal{E} \\ \mathcal{I} \end{bmatrix} \leq \mathcal{Y}\begin{bmatrix} \mathcal{E} \\ \mathcal{I} \end{bmatrix},$$

then, we have

$$\mathcal{Y} = \begin{bmatrix} -(\phi_1 + \rho) & 0 \\ \rho & -(\phi_1 + \gamma + \sigma) \end{bmatrix}. \quad \square$$

4. Description of HP-$\mathcal{ZZ}$TM to the general fractional DE

Here, we demonstrate the main idea of the HP-$\mathcal{ZZ}$TM, so we let the following general dynamical fractional non-homogeneous partial DE:

$$^{ABC}D_{\zeta}^{\wp}\mathcal{G}(\varkappa,\zeta) + \mathbb{R}\mathcal{G}(\varkappa,\zeta) + \mathbb{N}\mathcal{G}(\varkappa,\zeta) = F_1(\varkappa,\zeta), \tag{4.1}$$

supplemented by the initial conditions (ICs):

$$\mathcal{G}(\varkappa,0) = h_1(\varkappa) \quad and \quad f_{\zeta}(\varkappa,0) = l_1(\varkappa), \tag{4.2}$$

where $\mathbb{R}$ signifies the differential linear functional and $\mathbb{N}$ indicates the nonlinear factor, while $F_1(\varkappa,\zeta)$ represents the source factor. Employing $\mathcal{ZZ}$ transformation on both sides of (4.1), we have

$$\mathcal{Z}[\,^{ABC}D_{\zeta}^{\wp}\mathcal{G}(\varkappa,\zeta)] + \mathcal{Z}\{\mathbb{R}\,\mathcal{G}(\varkappa,\zeta)\} + \mathcal{Z}\{\mathbb{N}\mathcal{G}(\varkappa,\zeta)\} = \mathcal{Z}\{F_1(\varkappa,\zeta)\}. \tag{4.3}$$

Applying the differentiation rule to the aforesaid transform, we have

$$\mathcal{Z}[\mathcal{G}(\varkappa,\zeta)] = h_1(\varkappa) + \frac{\varpi}{\varphi}l_1(\varkappa) - \left(\frac{1-\wp}{\Lambda(\wp)} + \frac{\wp}{\Lambda(\wp)}\left(\frac{\varpi}{\varphi}\right)^{\wp}\right)\mathcal{Z}\Big[F_1(\varkappa,\zeta) - \mathbb{R}\mathcal{G}(\varkappa,\zeta) - \mathbb{N}\mathcal{G}(\varkappa,\zeta)\Big]. \tag{4.4}$$

Implementing the inverse $\mathcal{ZZ}$ transformation on both sides of (4.4) and using (4.2), then we get

$$\mathcal{G}(\varkappa,\zeta) = \mathcal{J}(\varkappa,\zeta) - \mathcal{Z}^{-1}\left[\left(\frac{1-\wp}{\Lambda(\wp)} + \frac{\wp}{\Lambda(\wp)}\left(\frac{\varpi}{\varphi}\right)^{\wp}\right)\mathcal{Z}[\mathcal{R}\mathcal{G}(\varkappa,\zeta) - \mathcal{N}\mathcal{G}(\varkappa,\zeta)]\right], \tag{4.5}$$

where $\mathcal{J}(\varkappa,\zeta)$ is defined to be the non-homogeneous term in the aforesaid (4.5). Now, we implement the HPM [54,55]. Moreover, we address the outcome with the aid of the HPM as a power series in the form of ε, as demonstrated below:

$$\mathcal{G}(\varkappa,\zeta) = \sum_{\mathrm{n}=0}^{\infty}\varepsilon^{\mathrm{n}}\mathcal{G}_{\mathrm{n}}(\varkappa,\zeta). \tag{4.6}$$

Furthermore, we classify the nonlinear term into

$$\mathbb{N}\mathcal{G}(\varkappa,\zeta) = \sum_{\mathrm{n}=0}^{\infty}\varepsilon^{\mathrm{n}}\Omega_{\mathrm{n}}(\mathcal{G}). \tag{4.7}$$

Ω_{n} are the He polynomials [56], which can be estimated using the following formulation:

$$\Omega_{\mathrm{n}}(\mathcal{G}_0,..,\mathcal{G}_{\mathrm{n}}) = \frac{1}{\mathrm{n}!}\frac{\partial^{\mathrm{n}}}{\partial\varepsilon^{\mathrm{n}}}\left(\mathbb{N}\Big(\sum_{\mathrm{n}=0}^{\infty}\varepsilon^{l}\mathcal{G}_{l}\Big)\right)_{\varepsilon=0}, \quad \mathrm{n} = 0,1,2,3,\ldots. \tag{4.8}$$

Plugging (4.6) and (4.7) into (4.5), we get

$$\sum_{\mathrm{n}=0}^{\infty}\varepsilon^{\mathrm{n}}\mathcal{G}_{\mathrm{n}} = \mathcal{J}(\varkappa,\zeta) - \left[(\mathcal{Z}^{-1}\left[\left(\frac{1-\wp}{\Lambda(\wp)} + \frac{\wp}{\Lambda(\wp)}\right)\left(\frac{\varpi}{\varphi}\right)^{\wp}\right]\mathcal{Z}\left[\mathbb{R}\sum_{\mathrm{n}=0}^{\infty}\varepsilon^{\mathrm{n}}\mathcal{G}_{\mathrm{n}} + \sum_{\mathrm{n}=0}^{\infty}\varepsilon^{\mathrm{n}}\Omega_{\mathrm{n}}(\mathcal{G})\right]\right]. \tag{4.9}$$

The aforesaid technique (4.9) is a convolution of the HPM and the $\mathcal{ZZ}$ transform. Now, by equating each side of (4.9) with respect to the power of ε, we get the initial approximation as follows:

$$\begin{aligned}
\varepsilon^0 &: \mathcal{G}_0(\varkappa,\zeta) = \mathcal{J}(\varkappa,\zeta),\\
\varepsilon^1 &: \mathcal{G}(\varkappa,\zeta) = -\mathcal{Z}^{-1}\left[\left(\frac{1-\wp}{\Lambda(\wp)} + \frac{\wp}{\Lambda(\wp)}\left(\frac{\varpi}{\varphi}\right)^{\wp}\right)\mathcal{Z}\left[\mathbb{R}\mathcal{G}_0(\varkappa,\zeta) + \Omega_0(\mathcal{G})\right]\right],\\
\varepsilon^2 &: \mathcal{G}_2(\varkappa,\zeta) = -\mathcal{Z}^{-1}\left[\left(\frac{1-\wp}{\Lambda(\wp)} + \frac{\wp}{\Lambda(\wp)}\left(\frac{\varpi}{\varphi}\right)^{\wp}\right)\mathcal{Z}\left[\mathbb{R}\mathcal{G}_1(\varkappa,\zeta) + \Omega_1(\mathcal{G})\right]\right],\\
\varepsilon^3 &: \mathcal{G}_3(\varkappa,\zeta) = -\mathcal{Z}^{-1}\left[\left(\frac{1-\wp}{\Lambda(\wp)} + \frac{\wp}{\Lambda(\wp)}\left(\frac{\varpi}{\varphi}\right)^{\wp}\right)\mathcal{Z}\left[\mathbb{R}\mathcal{G}_2(\varkappa,\zeta) + \Omega_2(\mathcal{G})\right]\right],\\
&\vdots
\end{aligned}$$

As a result, the series solution is expressed as follows:

$$\mathcal{G}(\varkappa,\zeta)=\mathcal{G}_0(\varkappa,\zeta)+\mathcal{G}_1(\varkappa,\zeta)+\mathcal{G}_2(\varkappa,\zeta)+\ldots.$$

4.1. Existence-uniqueness via fixed point theory

In what follows, the existence and uniqueness of the WP model (3.2) can be demonstrated as:
Here, $\mathcal{Z}(X)$ is used to indicate a Banach space, where $\mathcal{X}=[0,b]$ and $\mathcal{Y}=\mathcal{Z}(X)\times\mathcal{Z}(X)\times\mathcal{Z}(X)\times\mathcal{Z}(X)\times\mathcal{Z}(X)\times\mathcal{Z}(X)$ and the given norm $\|(\Omega_S,\Omega_\mathcal{E},\Omega_I,\Omega_R,\Omega_\mathcal{V})\| =\|\Omega_S\|+\|\Omega_\mathcal{E}\|+\|\Omega_I\|+\|\Omega_\mathcal{R}\|+\|\Omega_\mathcal{V}\|$, where $\Omega_S=sup_{\zeta\in X}\Omega_S$, $\Omega_\mathcal{E}=sup_{\zeta\in X}\Omega_\mathcal{E},\Omega_I=sup_{\zeta\in X}\Omega_I$, $\Omega_\mathcal{R}=sup_{\zeta\in X}\Omega_\mathcal{R}$, $\Omega_\mathcal{V}=sup_{\zeta\in X}\Omega_\mathcal{V}$, and applying the Definition 2.3 on worms propagation model (3.2), yields

$$\begin{aligned}
\|\Phi_{\Omega_{S_n}}(\zeta)\| &\le \frac{1-\wp}{\Lambda(\wp)}\mathcal{F}_1\|\Phi_{\Omega_{S_{n-1}}}(\zeta)\|\frac{\wp}{\Lambda(\wp)\Gamma(\wp)}\mathcal{F}_1\times\int_0^\zeta(\zeta-\theta)^{\wp-1}\|\Phi_{\Omega_{S_{n-1}}}(\zeta)\|d\theta,\\
\|\Phi_{\Omega_{\mathcal{E}_n}}(\zeta)\| &\le \frac{1-\wp}{\Lambda(\wp)}\mathcal{F}_2\|\Phi_{\Omega_{\mathcal{E}_{n-1}}}(\zeta)\|\frac{\wp}{\Lambda(\wp)\Gamma(\wp)}\mathcal{F}_2\times\int_0^\zeta(\zeta-\theta)^{\wp-1}\|\Phi_{\Omega_{\mathcal{E}_{n-1}}}(\zeta)\|d\theta,\\
\|\Phi_{\Omega_{I_n}}(\zeta)\| &\le \frac{1-\wp}{\Lambda(\wp)}\mathcal{F}_3\|\Phi_{\Omega_{I_{n-1}}}(\zeta)\|\frac{\wp}{\Lambda(\wp)\Gamma(\wp)}\mathcal{F}_3\times\int_0^\zeta(\zeta-\theta)^{\wp-1}\|\Phi_{\Omega_{I_{n-1}}}(\zeta)\|d\theta,\\
\|\Phi_{\Omega_{\mathcal{R}_n}}(\zeta)\| &\le \frac{1-\wp}{\Lambda(\wp)}\mathcal{F}_4\|\Phi_{\Omega_{\mathcal{R}_{n-1}}}(\zeta)\|\frac{\wp}{\Lambda(\wp)\Gamma(\wp)}\mathcal{F}_4\times\int_0^\zeta(\zeta-\theta)^{\wp-1}\|\Phi_{\Omega_{\mathcal{R}_{n-1}}}(\zeta)\|d\theta,\\
\|\Phi_{\Omega_{\mathcal{V}_n}}(\zeta)\| &\le \frac{1-\wp}{\Lambda(\wp)}\mathcal{F}_5\|\Phi_{\Omega_{\mathcal{V}_{n-1}}}(\zeta)\|\frac{\wp}{\Lambda(\wp)\Gamma(\wp)}\mathcal{F}_5\times\int_0^\zeta(\zeta-\theta)^{\wp-1}\|\Phi_{\Omega_{\mathcal{V}_{n-1}}}(\zeta)\|d\theta.
\end{aligned}\tag{4.10}$$

Again, making the use of Definition 2.3, we have

$$\begin{aligned}
\Omega_S(\zeta)-\Omega_S(0) &= \frac{1-\wp}{\Lambda(\wp)}\Phi_1\big(\zeta,\Omega_S(\zeta)\big)+\frac{\wp}{\Lambda(\wp)\Gamma(\wp)}\times\int_0^\zeta(\zeta-\theta)^{\wp-1}\Phi_1\big(\theta,\Omega_S(\theta)\big)d\theta,\\
\Omega_\mathcal{E}(\zeta)-\Omega_\mathcal{E}(0) &= \frac{1-\wp}{\Lambda(\wp)}\Phi_2\big(\zeta,\Omega_\mathcal{E}(\zeta)\big)+\frac{\wp}{\Lambda(\wp)\Gamma(\wp)}\times\int_0^\zeta(\zeta-\theta)^{\wp-1}\Phi_2\big(\theta,\Omega_\mathcal{E}(\theta)\big)d\theta,\\
\Omega_I(\zeta)-\Omega_I(0) &= \frac{1-\wp}{\Lambda(\wp)}\Phi_3\big(\zeta,\Omega_I(\zeta)\big)+\frac{\wp}{\Lambda(\wp)\Gamma(\wp)}\times\int_0^\zeta(\zeta-\theta)^{\wp-1}\Phi_3\big(\theta,\Omega_I(\theta)\big)d\theta,\\
\Omega_\mathcal{R}(\zeta)-\Omega_\mathcal{R}(0) &= \frac{1-\wp}{\Lambda(\wp)}\Phi_4\big(\zeta,\Omega_\mathcal{R}(\zeta)\big)+\frac{\wp}{\Lambda(\wp)\Gamma(\wp)}\times\int_0^\zeta(\zeta-\theta)^{\wp-1}\Phi_4\big(\theta,\Omega_\mathcal{R}(\theta)\big)d\theta,\\
\Omega_\mathcal{V}(\zeta)-\Omega_\mathcal{V}(0) &= \frac{1-\wp}{\Lambda(\wp)}\Phi_5\big(\zeta,\Omega_\mathcal{V}(\zeta)\big)+\frac{\wp}{\Lambda(\wp)\Gamma(\wp)}\times\int_0^\zeta(\zeta-\theta)^{\wp-1}\Phi_5\big(\theta,\Omega_\mathcal{V}(\theta)\big)d\theta.
\end{aligned}\tag{4.11}$$

Thus, we have

$$\begin{aligned}
\Phi_1\big(\theta,\Omega_S(\zeta)\big) &= \Delta-\lambda^\wp\Omega_S(\zeta)\Omega_I(\zeta)-(\phi_1^\wp+\phi_2^\wp)\Omega_S(\zeta)+\vartheta_1^\wp\Omega_\mathcal{R}(\zeta)+\vartheta_2^\wp\Omega_\mathcal{V}(\zeta),\\
\Phi_2\big(\theta,\Omega_\mathcal{E}(\zeta)\big) &= \lambda^\wp\Omega_S(\zeta)\Omega_I(\zeta)-(\phi_1^\wp+\rho^\wp)\Omega_\mathcal{E}(\zeta),\\
\Phi_3\big(\theta,\Omega_I(\zeta)\big) &= \rho^\wp\Omega_\mathcal{E}(\zeta)-(\phi_1^\wp+\gamma^\wp+\sigma^\wp)\Omega_I(\zeta),\\
\Phi_4\big(\theta,\Omega_\mathcal{R}(\zeta)\big) &= \sigma^\wp\Omega_I(\zeta)-(\phi_1^\wp+\vartheta_1^\wp)\Omega_\mathcal{R}(\zeta),\\
\Phi_5\big(\theta,\Omega_\mathcal{V}(\zeta)\big) &= \phi_2^\wp\Omega_S(\zeta)-(\phi_1^\wp+\vartheta_2^\wp)\Omega_\mathcal{V}(\zeta).
\end{aligned}\tag{4.12}$$

Furthermore, the ABC derivative operator only satisfies the Lipschitz condition [51].
In this scenario, $\Omega_S(\zeta)$, $\Omega_\mathcal{E}(\zeta)$, $\Omega_I(\zeta)$, $\Omega_\mathcal{R}(\zeta)$, *and* $\Omega_\mathcal{V}(\zeta)$ are upper bounds. Given that the pair of functions $\Omega_S(\zeta)$ *and* $\Omega_{S^*}(\zeta)$ exist only if

$$\|\Phi_1\left(\theta,\Omega_S(\zeta)\right)-\Phi_1\left(\theta,\Omega_S^*(\zeta)\right)\|=\left[\lambda^{\wp}\Omega_I^{\wp}(\zeta)+(\phi_1^{\wp}+\phi_2^{\wp})\right]\|\Omega_S(\zeta)-\Omega_S^*(\zeta)\|, \tag{4.13}$$

where $\mathcal{F}_1=|\lambda^{\wp}\Omega_I(\zeta)+(\phi_1^{\wp}+\phi_2^{\wp})|$.
Now, (4.13) reduces to

$$\|\Phi_1\left(\theta,\Omega_S(\zeta)\right)-\Phi_1\left(\theta,\Omega_S^*(\zeta)\right)\|\leq\mathcal{F}_1\|(\Omega_S(\zeta)-\Omega_S^*(\zeta))\|. \tag{4.14}$$

In the same manner, one can find

$$\begin{aligned}
&\|\Phi_2\left(\theta,\Omega_\mathcal{E}(\zeta)\right)-\Phi_2\left(\theta,\Omega_\mathcal{E}^*(\zeta)\right)\|\leq\mathcal{F}_2\|(\Omega_\mathcal{E}(\zeta)-\Omega_\mathcal{E}^*(\zeta))\|,\\
&\|\Phi_3\left(\theta,\Omega_I(\zeta)\right)-\Phi_3\left(\theta,\Omega_I^*(\zeta)\right)\|\leq\mathcal{F}_3\|(\Omega_I(\zeta)-\Omega_I^*(\zeta))\|,\\
&\|\Phi_4\left(\theta,\Omega_\mathcal{R}(\zeta)\right)-\Phi_4\left(\theta,\Omega_\mathcal{R}^*(\zeta)\right)\|\leq\mathcal{F}_4\|(\Omega_\mathcal{R}(\zeta)-\Omega_\mathcal{R}^*(\zeta))\|,\\
&\|\Phi_5\left(\theta,\Omega_\mathcal{V}(\zeta)\right)-\Phi_5\left(\theta,\Omega_\mathcal{V}^*(\zeta)\right)\|\leq\mathcal{F}_5\|(\Omega_\mathcal{V}(\zeta)-\Omega_\mathcal{V}^*(\zeta))\|,
\end{aligned} \tag{4.15}$$

where

$$\begin{aligned}
\mathcal{F}_2&=|\phi_1^{\wp}+\rho^{\wp}|,\\
\mathcal{F}_3&=|\phi_1^{\wp}+\gamma^{\wp}+\sigma^{\wp}|,\\
\mathcal{F}_4&=|\phi_1^{\wp}+\vartheta_1^{\wp}|,\\
\mathcal{F}_5&=|\phi_1^{\wp}+\vartheta_2^{\wp}|.
\end{aligned} \tag{4.16}$$

Since Lipschitz's criteria are satisfied. Now, again, consider the result of (4.11) as

$$\begin{aligned}
\Omega_{S_n}(\zeta)-\Omega_S(0)&=\frac{1-\wp}{\Lambda(\wp)}\Phi_1\left(\zeta,\Omega_{S_{n-1}}(\zeta)\right)+\frac{\wp}{\Lambda(\wp)\Gamma(\wp)}\times\int_0^\zeta(\zeta-\theta)^{\wp-1}\Phi_1\left(\theta,\Omega_{S_{n-1}}(\theta)\right)d\theta,\\
\Omega_{\mathcal{E}_n}(\zeta)-\Omega_\mathcal{E}(0)&=\frac{1-\wp}{\Lambda(\wp)}\Phi_2\left(\zeta,\Omega_{\mathcal{E}_{n-1}}(\zeta)\right)+\frac{\wp}{\Lambda(\wp)\Gamma(\wp)}\times\int_0^\zeta(\zeta-\theta)^{\wp-1}\Phi_2\left(\theta,\Omega_{\mathcal{E}_{n-1}}(\theta)\right)d\theta,\\
\Omega_{I_n}(\zeta)-\Omega_I(0)&=\frac{1-\wp}{\Lambda(\wp)}\Phi_3\left(\zeta,\Omega_{I_{n-1}}(\zeta)\right)+\frac{\wp}{\Lambda(\wp)\Gamma(\wp)}\times\int_0^\zeta(\zeta-\theta)^{\wp-1}\Phi_3\left(\theta,\Omega_{I_{n-1}}(\theta)\right)d\theta,\\
\Omega_{\mathcal{R}_n}(\zeta)-\Omega_\mathcal{R}(0)&=\frac{1-\wp}{\Lambda(\wp)}\Phi_4\left(\zeta,\Omega_{\mathcal{R}_{n-1}}(\zeta)\right)+\frac{\wp}{\Lambda(\wp)\Gamma(\wp)}\times\int_0^\zeta(\zeta-\theta)^{\wp-1}\Phi_4\left(\theta,\Omega_{\mathcal{R}_{n-1}}(\theta)\right)d\theta,\\
\Omega_{\mathcal{V}_n}(\zeta)-\Omega_\mathcal{V}(0)&=\frac{1-\wp}{\Lambda(\wp)}\Phi_5\left(\zeta,\Omega_{\mathcal{V}_{n-1}}(\zeta)\right)+\frac{\wp}{\Lambda(\wp)\Gamma(\wp)}\times\int_0^\zeta(\zeta-\theta)^{\wp-1}\Phi_5\left(\theta,\Omega_{\mathcal{V}_{n-1}}(\theta)\right)d\theta,
\end{aligned}$$

subject to the ICs:

$$\Omega_S(0)=\Omega_{S_0},\Omega_\mathcal{E}(0)=\Omega_{\mathcal{E}_0},\Omega_I(0)=\Omega_{I_0},\Omega_\mathcal{R}(0)=\Omega_{\mathcal{R}_0},\Omega_\mathcal{V}(0)=\Omega_{\mathcal{V}_0}.$$

The difference between successive terms yields

$$\begin{aligned}
\Omega_{S_n}(\zeta)=\sum_{i=0}^{n}\Phi_{\Omega_{S_n}}(\zeta),\Omega_{\mathcal{E}_n}(\zeta)=\sum_{i=0}^{n}\Phi_{\Omega_{\mathcal{E}_n}}(\zeta),\Omega_{I_n}(\zeta)=\sum_{i=0}^{n}\Phi_{\Omega_{I_n}}(\zeta),\\
\Omega_{\mathcal{R}_n}(\zeta)=\sum_{i=0}^{n}\Phi_{\Omega_{\mathcal{R}_n}}(\zeta),\Omega_{\mathcal{V}_n}(\zeta)=\sum_{i=0}^{n}\Phi_{\Omega_{\mathcal{V}_n}}(\zeta).
\end{aligned} \tag{4.17}$$

Making the use of (4.14)-(4.15), we have
$\Phi_{\Omega_{S_{n-1}}} = \Omega_{S_{n-1}}(\zeta) - \Omega_{S_{n-2}}(\zeta)$, $\Phi_{\Omega_{\mathcal{E}_{n-1}}} = \Omega_{\mathcal{E}_{n-1}}(\zeta) - \Omega_{\mathcal{E}_{n-2}}(\zeta)$, $\Phi_{\Omega_{I_{n-1}}} = \Omega_{I_{n-1}}(\zeta) - \Omega_{I_{n-2}}(\zeta)$, $\Phi_{\Omega_{\mathcal{R}_{n-1}}} = \Omega_{\mathcal{R}_{n-1}}(\zeta) - \Omega_{\mathcal{R}_{n-2}}(\zeta)$, $\Phi_{\Omega_{\mathcal{V}_{n-1}}} = \Omega_{\mathcal{V}_{n-1}}(\zeta) - \Omega_{\mathcal{V}_{n-2}}(\zeta)$,

$$\Phi_{\Omega_{S_n}}(\zeta) = \Omega_{S_n}(\zeta) - \Omega_{S_{n-1}}(\zeta) = \begin{cases} \frac{1-\wp}{\Lambda(\wp)}\Phi_1\left(\zeta, \Omega_{S_{n-1}}(\zeta)\right) - \frac{1-\wp}{\Lambda(\wp)}\Phi_1\left(\zeta, \Omega_{S_{n-2}}(\zeta)\right) \\ + \frac{\wp}{\Lambda(\wp)\Gamma(\wp)} \times \int_0^\zeta (\zeta-\theta)^{\wp-1}\Phi_1\left(\theta, \Omega_{S_{n-1}}(\theta)\right)d\theta \\ + \frac{\wp}{\Lambda(\wp)\Gamma(\wp)} \times \int_0^\zeta (\zeta-\theta)^{\wp-1}\Phi_1\left(\theta, \Omega_{S_{n-2}}(\theta)\right)d\theta, \end{cases}$$

$$\Phi_{\Omega_{\mathcal{E}_n}}(\zeta) = \Omega_{\mathcal{E}_n}(\zeta) - \Omega_{\mathcal{E}_{n-1}}(\zeta) = \begin{cases} \frac{1-\wp}{\Lambda(\wp)}\Phi_1\left(\zeta, \Omega_{\mathcal{E}_{n-1}}(\zeta)\right) - \frac{1-\wp}{\Lambda(\wp)}\Phi_2\left(\zeta, \Omega_{\mathcal{E}_{n-2}}(\zeta)\right) \\ + \frac{\wp}{\Lambda(\wp)\Gamma(\wp)} \times \int_0^\zeta (\zeta-\theta)^{\wp-1}\Phi_2\left(\theta, \Omega_{\mathcal{E}_{n-1}}(\theta)\right)d\theta \\ + \frac{\wp}{\Lambda(\wp)\Gamma(\wp)} \times \int_0^\zeta (\zeta-\theta)^{\wp-1}\Phi_2\left(\theta, \Omega_{\mathcal{E}_{n-2}}(\theta)\right)d\theta, \end{cases}$$

$$\Phi_{\Omega_{I_n}}(\zeta) = \Omega_{I_n}(\zeta) - \Omega_{I_{n-1}}(\zeta) = \begin{cases} \frac{1-\wp}{\Lambda(\wp)}\Phi_1\left(\zeta, \Omega_{I_{n-1}}(\zeta)\right) - \frac{1-\wp}{\Lambda(\wp)}\Phi_3\left(\zeta, \Omega_{I_{n-2}}(\zeta)\right) \\ + \frac{\wp}{\Lambda(\wp)\Gamma(\wp)} \times \int_0^\zeta (\zeta-\theta)^{\wp-1}\Phi_3\left(\theta, \Omega_{I_{n-1}}(\theta)\right)d\theta \\ + \frac{\wp}{\Lambda(\wp)\Gamma(\wp)} \times \int_0^\zeta (\zeta-\theta)^{\wp-1}\Phi_3\left(\theta, \Omega_{I_{n-2}}(\theta)\right)d\theta, \end{cases}$$

$$\Phi_{\Omega_{\mathcal{R}_n}}(\zeta) = \Omega_{\mathcal{R}_n}(\zeta) - \Omega_{\mathcal{R}_{n-1}}(\zeta) = \begin{cases} \frac{1-\wp}{\Lambda(\wp)}\Phi_1\left(\zeta, \Omega_{\mathcal{R}_{n-1}}(\zeta)\right) - \frac{1-\wp}{\Lambda(\wp)}\Phi_4\left(\zeta, \Omega_{\mathcal{R}_{n-2}}(\zeta)\right) \\ + \frac{\wp}{\Lambda(\wp)\Gamma(\wp)} \times \int_0^\zeta (\zeta-\theta)^{\wp-1}\Phi_4\left(\theta, \Omega_{\mathcal{R}_{n-1}}(\theta)\right)d\theta \\ + \frac{\wp}{\Lambda(\wp)\Gamma(\wp)} \times \int_0^\zeta (\zeta-\theta)^{\wp-1}\Phi_4\left(\theta, \Omega_{\mathcal{R}_{n-2}}(\theta)\right)d\theta, \end{cases}$$

$$\Phi_{\Omega_{\mathcal{V}_n}}(\zeta) = \Omega_{\mathcal{V}_n}(\zeta) - \Omega_{\mathcal{V}_{n-1}}(\zeta) = \begin{cases} \frac{1-\wp}{\Lambda(\wp)}\Phi_5\left(\zeta, \Omega_{\mathcal{V}_{n-1}}(\zeta)\right) - \frac{1-\wp}{\Lambda(\wp)}\Phi_5\left(\zeta, \Omega_{\mathcal{V}_{n-2}}(\zeta)\right) \\ + \frac{\wp}{\Lambda(\wp)\Gamma(\wp)} \times \int_0^\zeta (\zeta-\theta)^{\wp-1}\Phi_5\left(\theta, \Omega_{\mathcal{V}_{n-1}}(\theta)\right)d\theta \\ + \frac{\wp}{\Lambda(\wp)\Gamma(\wp)} \times \int_0^\zeta (\zeta-\theta)^{\wp-1}\Phi_5\left(\theta, \Omega_{\mathcal{V}_{n-2}}(\theta)\right)d\theta. \end{cases} \tag{4.18}$$

Furthermore, we have

$$\|\Phi_{\Omega_{S_n}}(\zeta)\| \leq \frac{1-\wp}{\Lambda(\wp)}\mathcal{F}_1\|\Phi_{\Omega_{S_{n-1}}}(\zeta)\| \frac{\wp}{\Lambda(\wp)\Gamma(\wp)}\mathcal{F}_1 \times \int_0^\zeta (\zeta-\theta)^{\wp-1}\|\Phi_{\Omega_{S_{n-1}}}(\zeta)\|d\theta,$$

$$\|\Phi_{\Omega_{\mathcal{E}_n}}(\zeta)\| \leq \frac{1-\wp}{\Lambda(\wp)}\mathcal{F}_2\|\Phi_{\Omega_{\mathcal{E}_{n-1}}}(\zeta)\| \frac{\wp}{\Lambda(\wp)\Gamma(\wp)}\mathcal{F}_2 \times \int_0^\zeta (\zeta-r)^{\wp-1}\|\Phi_{\Omega_{\mathcal{E}_{n-1}}}(\zeta)\|d\theta,$$

$$\|\Phi_{\Omega_{I_n}}(\zeta)\| \leq \frac{1-\wp}{\Lambda(\wp)}\mathcal{F}_3\|\Phi_{\Omega_{I_{n-1}}}(\zeta)\| \frac{\wp}{\Lambda(\wp)\Gamma(\wp)}\mathcal{F}_3 \times \int_0^\zeta (\zeta-r)^{\wp-1}\|\Phi_{\Omega_{I_{n-1}}}(\zeta)\|d\theta,$$

$$\|\Phi_{\Omega_{\mathcal{R}_n}}(\zeta)\| \leq \frac{1-\wp}{\Lambda(\wp)}\mathcal{F}_4\|\Phi_{\Omega_{\mathcal{R}_{n-1}}}(\zeta)\| \frac{\wp}{\Lambda(\wp)\Gamma(\wp)}\mathcal{F}_4 \times \int_0^\zeta (\zeta-\theta)^{\wp-1}\|\Phi_{\Omega_{\mathcal{R}_{n-1}}}(\zeta)\|d\theta,$$

$$\|\Phi_{\Omega_{\mathcal{V}_n}}(\zeta)\| \leq \frac{1-\wp}{\Lambda(\wp)}\mathcal{F}_5\|\Phi_{\Omega_{\mathcal{V}_{n-1}}}(\zeta)\| \frac{\wp}{\Lambda(\wp)\Gamma(\wp)}\mathcal{F}_5 \times \int_0^\zeta (\zeta-r)^{\wp-1}\|\Phi_{\Omega_{\mathcal{V}_{n-1}}}(\zeta)\|d\theta. \tag{4.19}$$

Theorem 4.1. *Assume that WP model (3.2) has unique solution for $\zeta \in [0, \mathbf{c}_2]$ subject to the assumption $\frac{1-\wp}{\Lambda(\wp)}\phi_1 + \frac{\wp}{\Lambda(\wp)\Gamma(\wp)}\mathbf{c}_2^{\wp}$ $(n_i < 1,\ \ i = 1, ..., 5)$ holds.*

Proof. Assume that $\hat{\Omega}_S(\zeta), \hat{\Omega}_\mathcal{E}(\zeta), \hat{\Omega}_I(\zeta), \hat{\Omega}_\mathcal{R}(\zeta), \hat{\Omega}_\mathcal{V}(\zeta)$ is other solution of WP model (3.2).

Then by Definitions (2.3), we have

$$\|\Omega_{\mathcal{S}}(\zeta)-\widehat{\Omega}_{\mathcal{S}}(\zeta)\| \leq \frac{1-\wp}{\Lambda(\wp)}\phi_1\|\Omega_{\mathcal{S}}(\zeta)-\widehat{\Omega}_{\mathcal{S}}(\zeta)\| + \frac{\zeta\wp}{\Lambda(\wp)\Gamma(\wp)}\phi_1\|\Omega_{\mathcal{S}}(\zeta)-\widehat{\Omega}_{\mathcal{S}}(\zeta)\|. \tag{4.20}$$

Since $\left(\frac{1-\wp}{\Lambda(\wp)}-\frac{\zeta\wp}{\Lambda(\wp)\Gamma(\wp)}\right)>0$ satisfying that $\|\Omega_{\mathcal{S}}(\zeta)-\widehat{\Omega}_{\mathcal{S}}(\zeta)\|=0$. So that $\Omega_{\mathcal{S}}(\zeta)=\widehat{\Omega}_{\mathcal{S}}(\zeta)$.
In the similar manner, we can evaluate that $\Omega_{\mathcal{E}}(\zeta)=\widehat{\Omega}_{\mathcal{E}}(\zeta)$, $\Omega_{\mathcal{I}}(\zeta)=\widehat{\Omega}_{\mathcal{I}}(\zeta)$, $\Omega_{\mathcal{R}}(\zeta)=\widehat{\Omega}_{\mathcal{R}}(\zeta)$, $\Omega_{\mathcal{V}}(\zeta)=\widehat{\Omega}_{\mathcal{V}}(\zeta)$. This yields the intended outcome. □

5. Analytical solution of fractional WP model

Initially, we apply the $\mathcal{ZZ}$ transform to both sides of (3.2), we have

$$\begin{cases}
\mathcal{Z}[{}^{ABC}\mathcal{D}_{\zeta}^{\wp}\mathcal{S}(\zeta)] = \mathcal{Z}\left[\Delta\right]-\lambda\mathcal{Z}\left[\mathcal{S}(\zeta)\mathcal{I}(\zeta)\right]-(\phi_1+\phi_2)\mathcal{Z}\left[\mathcal{S}(\zeta)\right]+\vartheta_1\mathcal{Z}\left[\mathcal{R}(\zeta)\right]+\vartheta_2\mathcal{Z}\left[\mathcal{V}(\zeta)\right],\\
\mathcal{Z}[{}^{ABC}\mathcal{D}_{\zeta}^{\wp}\mathcal{E}(\zeta)] = \lambda\mathcal{Z}\left[\mathcal{S}(\zeta)\mathcal{I}(\zeta)\right]-(\phi_1+\rho)\mathcal{Z}\left[\mathcal{E}(\zeta)\right],\\
\mathcal{Z}[{}^{ABC}\mathcal{D}_{\zeta}^{\wp}\mathcal{I}(\zeta)] = \rho\mathcal{Z}\left[\mathcal{E}(\zeta)\right]-(\phi_1+\gamma+\sigma)\mathcal{Z}\left[\mathcal{I}(\zeta)\right],\\
\mathcal{Z}[{}^{ABC}\mathcal{D}_{\zeta}^{\wp}\mathcal{R}(\zeta)] = \sigma\mathcal{Z}\left[\mathcal{I}(\zeta)\right]-(\phi_1+\vartheta_1)\mathcal{Z}\left[\mathcal{R}(\zeta)\right],\\
\mathcal{Z}[{}^{ABC}\mathcal{D}_{\zeta}^{\wp}\mathcal{V}(\zeta)] = \phi_2\mathcal{Z}\left[\mathcal{S}(\zeta)\right]-(\phi_1+\vartheta_2)\mathcal{Z}\left[\mathcal{V}(\zeta)\right].
\end{cases} \tag{5.1}$$

It follows that

$$\begin{cases}
\mathcal{Z}\left[\mathcal{S}(\zeta)\right]_{=} \ \mathcal{S}(0)+\left(\frac{1-\wp}{\Lambda(\wp)}+\frac{\wp}{\Lambda(\wp)}(\frac{\varpi}{\varphi})^{\wp}\right)\Big(\mathcal{Z}\left[\Delta\right]-\lambda\mathcal{Z}\left[\mathcal{S}(\zeta)\mathcal{I}(\zeta)\right]-(\phi_1+\phi_2)\mathcal{Z}\left[\mathcal{S}(\zeta)\right]\\
\qquad\qquad +\vartheta_1\mathcal{Z}\left[\mathcal{R}(\zeta)\right]+\vartheta_2\mathcal{Z}\left[\mathcal{V}(\zeta)\right]\Big),\\
\mathcal{Z}\left[\mathcal{E}(\zeta)\right] = \ \mathcal{E}(0)+\left(\frac{1-\wp}{\Lambda(\wp)}+\frac{\wp}{\Lambda(\wp)}(\frac{\varpi}{\varphi})^{\wp}\right)\Big(\lambda\mathcal{Z}\left[\mathcal{S}(\zeta)\mathcal{I}(\zeta)\right]-(\phi_1+\rho)\mathcal{Z}\left[\mathcal{E}(\zeta)\right]\Big),\\
\mathcal{Z}\left[\mathcal{I}(\zeta)\right] = \ \mathcal{I}(0)+\left(\frac{1-\wp}{\Lambda(\wp)}+\frac{\wp}{\Lambda(\wp)}(\frac{\varpi}{\varphi})^{\wp}\right)\Big(\rho\mathcal{Z}\left[\mathcal{E}(\zeta)\right]-(\phi_1+\gamma+\sigma)\mathcal{Z}\left[\mathcal{I}(\zeta)\right]\Big),\\
\mathcal{Z}\left[\mathcal{R}(\zeta)\right] = \ \mathcal{R}(0)+\left(\frac{1-\wp}{\Lambda(\wp)}+\frac{\wp}{\Lambda(\wp)}(\frac{\varpi}{\varphi})^{\wp}\right)\Big(\sigma\mathcal{Z}\left[\mathcal{I}(\zeta)\right]-(\phi_1+\vartheta_1)\mathcal{Z}\left[\mathcal{R}(\zeta)\right]\Big),\\
\mathcal{Z}\left[\mathcal{V}(\zeta)\right] = \ \mathcal{V}(0)+\left(\frac{1-\wp}{\Lambda(\wp)}+\frac{\wp}{\Lambda(\wp)}(\frac{\varpi}{\varphi})^{\wp}\right)\Big(\phi_2\mathcal{Z}\left[\mathcal{S}(\zeta)\right]-(\phi_1+\vartheta_2)\mathcal{Z}\left[\mathcal{V}(\zeta)\right]\Big).
\end{cases} \tag{5.2}$$

Using the ICs (3.3), we take the inverse of $\mathcal{ZZ}$ transform on both sides of (5.2), we obtain

$$\begin{cases}
\mathcal{S}(\zeta) = \mathcal{W}_1+\mathcal{Z}^{-1}\left[\left(\frac{1-\wp}{\Lambda(\wp)}+\frac{\wp}{\Lambda(\wp)}(\frac{\varpi}{\varphi})^{\wp}\right)\left(\Delta-\lambda\mathcal{Z}\left[\mathcal{S}(\zeta)\mathcal{I}(\zeta)\right]-(\phi_1+\phi_2)\mathcal{Z}\left[\mathcal{S}(\zeta)\right]\right.\right.\\
\qquad\left.\left.+\vartheta_1\mathcal{Z}\left[\mathcal{R}(\zeta)\right]+\vartheta_2\mathcal{Z}\left[\mathcal{V}(\zeta)\right]\right)\right],\\
\mathcal{E}(\zeta) = \mathcal{W}_2+\mathcal{Z}^{-1}\left[\left(\frac{1-\wp}{\Lambda(\wp)}+\frac{\wp}{\Lambda(\wp)}(\frac{\varpi}{\varphi})^{\wp}\right)\left(\lambda\mathcal{Z}\left[\mathcal{S}(\zeta)\mathcal{I}(\zeta)\right]-(\phi_1+\rho)\mathcal{Z}\left[\mathcal{E}(\zeta)\right]\right)\right],\\
\mathcal{I}(\zeta) = \mathcal{W}_3+\mathcal{Z}^{-1}\left[\left(\frac{1-\wp}{\Lambda(\wp)}+\frac{\wp}{\Lambda(\wp)}(\frac{\varpi}{\varphi})^{\wp}\right)\left(\rho\mathcal{Z}\left[\mathcal{E}(\zeta)\right]-(\phi_1+\gamma+\sigma)\mathcal{Z}\left[\mathcal{I}(\zeta)\right]\right)\right],\\
\mathcal{R}(\zeta) = \mathcal{W}_4+\mathcal{Z}^{-1}\left[\left(\frac{1-\wp}{\Lambda(\wp)}+\frac{\wp}{\Lambda(\wp)}(\frac{\varpi}{\varphi})^{\wp}\right)\Big(\sigma\mathcal{Z}\left[\mathcal{I}(\zeta)\right]-(\phi_1+\vartheta_1)\mathcal{Z}\left[\mathcal{R}(\zeta)\right]\Big)\right],\\
\mathcal{V}(\zeta) = \mathcal{W}_5+\mathcal{Z}^{-1}\left[\left(\frac{1-\wp}{\Lambda(\wp)}+\frac{\wp}{\Lambda(\wp)}(\frac{\varpi}{\varphi})^{\wp}\right)\Big(\phi_2\mathcal{Z}\left[\mathcal{S}(\zeta)\right]-(\phi_1+\vartheta_2)\mathcal{Z}\left[\mathcal{V}(\zeta)\right]\Big)\right].
\end{cases} \tag{5.3}$$

We will present the results in the following infinite sequence.

$$\mathcal{S}(\mathrm{n})=\sum_{\mathrm{n}=0}^{\infty}\varepsilon^{\mathrm{n}}\mathcal{S}(\mathrm{n}),\quad \mathcal{E}(\mathrm{n})=\sum_{\mathrm{n}=0}^{\infty}\varepsilon^{\mathrm{n}}\mathcal{E}(\mathrm{n}),\quad \mathcal{I}(\mathrm{n})=\sum_{\mathrm{n}=0}^{\infty}\varepsilon^{\mathrm{n}}\mathcal{I}(\mathrm{n}),\quad \mathcal{R}(\mathrm{n})=\sum_{\mathrm{n}=0}^{\infty}\varepsilon^{\mathrm{n}}\mathcal{R}(\mathrm{n}),\quad \mathcal{V}(\mathrm{n})=\sum_{\mathrm{n}=0}^{\infty}\varepsilon^{\mathrm{n}}\mathcal{V}(\mathrm{n}), \tag{5.4}$$

as well as nonlinear terms such as

$$\sum_{\mathrm{n}=0}^{\infty}\varepsilon^{\mathrm{n}}\mathcal{H}_{\mathrm{n}}=\mathcal{S}\mathcal{I}. \tag{5.5}$$

If we replaced (5.3) and (5.4) with (5.2), we obtain

$$
\begin{cases}
\sum_{n=0}^{\infty}\varepsilon^{n}\mathcal{S}(n)=\mathcal{W}_1+\varepsilon\mathcal{Z}^{-1}\Big[\Big(\frac{1-\wp}{\Lambda(\wp)}+\frac{\wp}{\Lambda(\wp)}(\frac{\varpi}{\varphi})^{\wp}\Big)\mathcal{Z}\big[\Delta\big]\Big]\\
-\lambda\varepsilon\mathcal{Z}^{-1}\Big[\Big(\frac{1-\wp}{\Lambda(\wp)}+\frac{\wp}{\Lambda(\wp)}(\frac{\varpi}{\varphi})^{\wp}\Big)\mathcal{Z}\big[\sum_{n=0}^{\infty}\varepsilon^{n}\Omega_n\big]\Big]\\
-\varepsilon(\phi_1+\phi_2)\mathcal{Z}^{-1}\Big[\Big(\frac{1-\wp}{\Lambda(\wp)}+\frac{\wp}{\Lambda(\wp)}(\frac{\varpi}{\varphi})^{\wp}\Big)\big[\sum_{n=0}^{\infty}\varepsilon^{n}\mathcal{S}_n(\zeta)\big]\Big]\\
+\vartheta_1\varepsilon\mathcal{Z}^{-1}\Big[\Big(\frac{1-\wp}{\Lambda(\wp)}+\frac{\wp}{\Lambda(\wp)}(\frac{\varpi}{\varphi})^{\wp}\Big)\big[\sum_{n=0}^{\infty}\varepsilon^{n}\mathcal{R}_n(\zeta)\big]\Big]\\
+\varepsilon\vartheta_2\mathcal{Z}^{-1}\Big[\Big(\frac{1-\wp}{\Lambda(\wp)}+\frac{\wp}{\Lambda(\wp)}(\frac{\varpi}{\varphi})^{\wp}\Big)\big[\sum_{n=0}^{\infty}\varepsilon^{n}\mathcal{V}_n(\zeta)\big]\Big],\\
\sum_{n=0}^{\infty}\varepsilon^{n}\mathcal{E}(n)=\mathcal{W}_2+\varepsilon\lambda\mathcal{Z}^{-1}\Big[\big(\frac{1-\wp}{\Lambda(\wp)}+\frac{\wp}{\Lambda(\wp)_1}(\frac{\varpi}{\varphi})^{\wp}\big)\mathcal{Z}\big[\sum_{n=0}^{\infty}\varepsilon^{n}\Omega_n\big]\Big]\\
\qquad -\varepsilon(\phi_1+\rho)\mathcal{Z}^{-1}\Big[\big(\frac{1-\wp}{\Lambda(\wp)}+\frac{\wp}{\Lambda(\wp)}(\frac{\varpi}{\varphi})^{\wp}\big)\big[\sum_{n=0}^{\infty}\varepsilon^{n}\mathcal{E}_n(\zeta)\big]\Big],\\
\sum_{n=0}^{\infty}\varepsilon^{n}\mathcal{I}(n)=\mathcal{W}_3+\varepsilon\rho\mathcal{Z}^{-1}\Big[\big(\frac{1-\wp}{\Lambda(\wp)}+\frac{\wp}{\Lambda(\wp)}(\frac{\varpi}{\varphi})^{\wp}\big)\mathcal{Z}\big[\sum_{n=0}^{\infty}\varepsilon^{n}\mathcal{E}_n(\zeta)\big]\Big]\\
\qquad -\varepsilon(\phi_1+\gamma+\sigma)\mathcal{Z}^{-1}\Big[\big(\frac{1-\wp}{\Lambda(\wp)}+\frac{\wp}{\Lambda(\wp)}(\frac{\varpi}{\varphi})^{\wp}\big)\mathcal{Z}\big[\sum_{n=0}^{\infty}\varepsilon^{n}\mathcal{I}_n(\zeta)\big]\Big],\\
\sum_{n=0}^{\infty}\varepsilon^{n}\mathcal{R}(n)=\mathcal{W}_4+\varepsilon\sigma\mathcal{Z}^{-1}\Big[\big(\frac{1-\wp}{\Lambda(\wp)}+\frac{\wp}{\Lambda(\wp)}(\frac{\varpi}{\varphi})^{\wp}\big)\mathcal{Z}\big[\sum_{n=0}^{\infty}\varepsilon^{n}\mathcal{I}_n(\zeta)\big]\Big]\\
\qquad -\varepsilon(\phi_1+\vartheta_1)\mathcal{Z}^{-1}\Big[\big(\frac{1-\wp}{\Lambda(\wp)}+\frac{\wp}{\Lambda(\wp)}(\frac{\varpi}{\varphi})^{\wp}\big)\mathcal{Z}\big[\sum_{n=0}^{\infty}\varepsilon^{n}\mathcal{R}(\zeta)\big]\Big],\\
\sum_{n=0}^{\infty}\varepsilon^{n}\mathcal{V}(n)=\mathcal{W}_5+\varepsilon\phi_2\mathcal{Z}^{-1}\Big[\big(\frac{1-\wp}{\Lambda(\wp)}+\frac{\wp}{\Lambda(\wp)}(\frac{\varpi}{\varphi})^{\wp}\big)\mathcal{Z}\big[\sum_{n=0}^{\infty}\varepsilon^{n}\mathcal{S}(\zeta)\big]\Big]\\
\qquad -\varepsilon(\phi_1+\vartheta_2)\mathcal{Z}^{-1}\Big[\big(\frac{1-\wp}{\Lambda(\wp)}+\frac{\wp}{\Lambda(\wp)}(\frac{\varpi}{\varphi})^{\wp}\big)\mathcal{Z}\big[\sum_{n=0}^{\infty}\varepsilon^{n}\mathcal{V}(\zeta)\big]\Big].
\end{cases}
\tag{5.6}
$$

Considering few initial terms of He's polynomials' [56], we have

$$
\begin{aligned}
\mathcal{H}_0 &= \mathcal{W}_1\mathcal{W}_3,\\
\mathcal{H}_1 &= \Big[\frac{1-\wp}{\Lambda(\wp)}+\frac{\wp}{\Lambda(\wp)}\frac{\zeta^{\wp}}{\Gamma(\wp+1)}\Big]\\
&\quad\Big(\Delta\mathcal{W}_3-\lambda\mathcal{W}_1\mathcal{W}_3^2-(\phi_1+\phi_2)\mathcal{W}_1\mathcal{W}_3+\vartheta_1\mathcal{W}_4\mathcal{W}_3+\vartheta_2\mathcal{W}_5\mathcal{W}_3+\rho\mathcal{W}_2\mathcal{W}_1-(\phi_1+\gamma+\sigma)\mathcal{W}_1\mathcal{W}_3\Big),\\
\mathcal{H}_2 &= \frac{\mathcal{W}_3\Delta}{\Lambda(\wp)}\Big[1-\wp+\frac{\wp.\zeta^{\wp}}{\Gamma(\wp+1)}\Big]-\frac{1}{(\Lambda(\wp))^2}\Big[(1-\wp)^2+\frac{2\wp(1-\wp)(\zeta)^{\wp}}{\Gamma(\wp+1)}+\frac{\wp^2(t^{2\wp})}{\Gamma(2\wp+1)}\Big]\\
&\quad\times\begin{cases}\Big(\lambda\Delta\mathcal{W}_3^2-\lambda^2\mathcal{W}_1\mathcal{W}_3^3-(\phi_1+\phi_2)\lambda\mathcal{W}_1\mathcal{W}_3^2+\vartheta_1\lambda\mathcal{W}_3^2\mathcal{W}_4+\vartheta_2\lambda\mathcal{W}_3^2\mathcal{W}_5+\lambda\mathcal{W}_1\mathcal{W}_2\mathcal{W}_3\\
-\lambda(\phi_1+\gamma+\sigma)\mathcal{W}_1\mathcal{W}_3^2-(\phi_1+\phi_2)\Delta\mathcal{W}_3+\lambda(\phi_1+\phi_2)\mathcal{W}_1\mathcal{W}_3^2+(\phi_1+\phi_2)^2\mathcal{W}_1\mathcal{W}_3\\
-\vartheta_1(\phi_1+\phi_2)\mathcal{W}_3\mathcal{W}_4-\vartheta_2(\phi_1+\phi_2)\mathcal{W}_3\mathcal{W}_5+\sigma\vartheta_1\mathcal{W}_3^2-\vartheta_1(\phi_1+\vartheta_1)\mathcal{W}_3\mathcal{W}_4+\vartheta_2\phi_2\mathcal{W}_1\mathcal{W}_3\\
-\vartheta_2(\phi_1+\vartheta_2)\mathcal{W}_3\mathcal{W}_5\Big)\end{cases}\\
&\quad-\begin{cases}\Big(\big[\Delta\mathcal{W}_2-(\phi_1+\gamma+\sigma)\mathcal{W}_3\big]\times\big[\Delta-\lambda\mathcal{W}_1\mathcal{W}_3-(\phi_1+\phi_2)\mathcal{W}_1+\vartheta_1\mathcal{W}_4+\vartheta_2\mathcal{W}_5\big]\Big)\\
\quad+\Big(\big[\rho\lambda\mathcal{W}_1^2\mathcal{W}_3-(\phi_1+\rho)\rho\mathcal{W}_1\mathcal{W}_2-(\phi_1+\gamma+\sigma)\rho\mathcal{W}_1\mathcal{W}_2+(\phi_1+\gamma+\sigma)^2\mathcal{W}_1\mathcal{W}_3\big]\Big).\end{cases}\\
&\ \vdots\ .
\end{aligned}
$$

Plugging (5.6) and compared both sides of (5.5), we find

$$
\begin{aligned}
\mathcal{S}_0(\zeta) &= \mathcal{W}_1,\\
\mathcal{S}_1(\zeta) &= \Big[\frac{1-\wp}{\Lambda(\wp)}+\frac{\wp}{\Lambda(\wp)}\frac{\zeta^{\wp}}{\Gamma(\wp+1)}\Big]\Big(\Delta-\lambda\mathcal{W}_1\mathcal{W}_3-(\phi_1+\phi_2)\mathcal{W}_1+\vartheta_1\mathcal{W}_4+\vartheta_2\mathcal{W}_5\Big),\\
\mathcal{S}_2(\zeta) &= \frac{\Delta}{\Lambda(\wp)}\Big[1-\wp+\frac{\wp.\zeta^{\wp}}{\Gamma(\wp+1)}\Big]-\frac{1}{(\Lambda(\wp))^2}\Big[(1-\wp)^2+\frac{2\wp(1-\wp)(\zeta)^{\wp}}{\Gamma(\wp+1)}+\frac{\wp^2(t^{2\wp})}{\Gamma(2\wp+1)}\Big]
\end{aligned}
$$

$$\times\begin{cases}\Big(-\Delta\lambda\mathcal{W}_3+\lambda^2\mathcal{W}_1\mathcal{W}_3^2+(\phi_1+\phi_2)\lambda\mathcal{W}_1\mathcal{W}_3-\vartheta_1\lambda\mathcal{W}_3\mathcal{W}_4-\vartheta_2\lambda\mathcal{W}_3\mathcal{W}_5-\rho\lambda\mathcal{W}_1\mathcal{W}_2\\ +(\phi_1+\gamma+\sigma)\lambda\mathcal{W}_1\mathcal{W}_3+(\phi_1+\phi_2)\Delta-\lambda(\phi_1+\phi_2)\mathcal{W}_1\mathcal{W}_3-(\phi_1+\phi_2)^2\mathcal{W}_1+\vartheta_1(\phi_1+\phi_2)\mathcal{W}_4\\ +\vartheta_2(\phi_1+\phi_2)\mathcal{W}_5-\sigma\vartheta_1\mathcal{W}_3+\vartheta_1(\phi_1+\vartheta_1)\mathcal{W}_4-\vartheta_2\phi_2\mathcal{W}_1+\vartheta_2(\phi_1+\vartheta_2)\mathcal{W}_5\Big),\end{cases}$$

$$\mathcal{S}_3(\zeta)=\frac{\Delta}{\Lambda(\wp)}\left[1-\wp+\frac{\wp\zeta^{\wp}}{\Gamma(\wp+1)}\right]-\frac{\Delta}{(\Lambda(\wp))^2}\left[(1-\wp)^2+\frac{2\wp(1-\wp)(\zeta)^{\wp}}{\Gamma(\wp+1)}+\frac{\wp^2(\zeta^{2\wp})}{\Gamma(2\wp+1)}\right].\Big(\lambda\mathcal{W}_3+(\phi_1+\phi_2)\Big)$$

$$+\frac{1}{(\Lambda(\wp))^3}\left[(1-\wp)^3+\frac{3\wp(1-\wp)^2(\zeta)^{\wp}}{\Gamma(\wp+1)}+\frac{3\wp^2(1-\wp)(t^{2\wp})}{\Gamma(2\wp+1)}+\frac{\wp^3\zeta^{3\wp}}{\Gamma(3\wp+1)}\right]$$

$$\times\begin{cases}\Big(\rho\lambda^2\mathcal{W}_1\mathcal{W}_2\mathcal{W}_3-(\phi_1+\gamma+\sigma)\lambda^2\mathcal{W}_1\mathcal{W}_3^2+\Delta\lambda^2\mathcal{W}_3^2+\lambda^3\mathcal{W}_1\mathcal{W}_3^3-(\phi_1+\phi_2)\lambda^2\mathcal{W}_1\mathcal{W}_3^2\\ -\vartheta_1\lambda^2\mathcal{W}_3^2\mathcal{W}_4+\vartheta_2\lambda^2\mathcal{W}_3^2\mathcal{W}_5-\Delta\lambda(\phi_1+\phi_2)\mathcal{W}_3+\lambda^2(\phi_1+\phi_2)\mathcal{W}_1\mathcal{W}_3^2+\lambda(\phi_1+\phi_2)^2\mathcal{W}_1\mathcal{W}_3\\ -\vartheta_1\lambda(\phi_1+\phi_2)\mathcal{W}_3\mathcal{W}_4-\vartheta_2\lambda(\phi_1+\phi_2)\mathcal{W}_3\mathcal{W}_5+\vartheta_1\sigma\lambda\mathcal{W}_3^2-\vartheta_1\lambda(\phi_1+\vartheta_1)\mathcal{W}_3\mathcal{W}_4+\lambda\vartheta_2\phi_2\mathcal{W}_1\mathcal{W}_3\\ -(\phi_1+\vartheta_1)\vartheta_2\lambda\mathcal{W}_3\mathcal{W}_5\Big)\end{cases}$$

$$-\begin{cases}+\Big(\Big[\Delta\lambda-\lambda^2\mathcal{W}_1\mathcal{W}_3-\lambda(\phi_1+\phi_2)\mathcal{W}_1+\vartheta_1\lambda\mathcal{W}_4+\vartheta_2\lambda\mathcal{W}_5\Big].\Big[\Delta\lambda\mathcal{W}_2-(\phi_1+\gamma+\sigma)\lambda\mathcal{W}_3\Big]\Big)\\ \quad+\Big(\rho\lambda^2\mathcal{W}_1^2\mathcal{W}_3-(\phi_1+\rho)\rho\lambda\mathcal{W}_1\mathcal{W}_2-(\phi_1+\gamma+\sigma)\rho\lambda\mathcal{W}_1\mathcal{W}_2+(\phi_1+\gamma+\sigma)^2\lambda\mathcal{W}_1\mathcal{W}_3\Big)\end{cases}$$

$$+\begin{cases}\Big(-(\phi_1+\phi_2)\rho\lambda\mathcal{W}_1\mathcal{W}_2+(\phi_1+\phi_2)(\phi_1+\gamma+\sigma)\lambda\mathcal{W}_1\mathcal{W}_3-(\phi_1+\phi_2)\Delta\lambda\mathcal{W}_3+(\phi_1+\phi_2)\lambda^2\mathcal{W}_3^2\mathcal{W}_1\\ +(\phi_1+\phi_2)^2\lambda\mathcal{W}_1\mathcal{W}_3-(\phi_1+\phi_2)\vartheta_1\lambda\mathcal{W}_3\mathcal{W}_4-(\phi_1+\phi_2)\vartheta_2\lambda\mathcal{W}_3\mathcal{W}_5+\Delta(\phi_1+\phi_2)^2-(\phi_1+\phi_2)^2\lambda\mathcal{W}_1\mathcal{W}_3\\ -(\phi_1+\phi_2)^3\mathcal{W}_1+(\phi_1+\phi_2)^2\vartheta_1\mathcal{W}_4+(\phi_1+\phi_2)^2\vartheta_2\mathcal{W}_5-(\phi_1+\phi_2)\vartheta_1\sigma\mathcal{W}_3+(\phi_1+\phi_2)(\phi_1+\vartheta_1)\vartheta_1\mathcal{W}_4\\ -(\phi_1+\phi_2)\vartheta_2\phi_2\mathcal{W}_1+(\phi_1+\vartheta_2)(\phi_1+\phi_2)\vartheta_2\mathcal{W}_5\Big)\end{cases}$$

$$+\begin{cases}\Big(\vartheta_1\sigma\rho\mathcal{W}_2-\vartheta_1\sigma(\phi_1+\gamma+\sigma)\mathcal{W}_3-\vartheta_1\sigma(\phi_1+\vartheta_1)\mathcal{W}_3+\vartheta_1(\phi_1+\vartheta_1)^2\mathcal{W}_4\Big)\\ \quad+\Big(\vartheta_2\Delta\phi_2-\vartheta_2\lambda\phi_2\mathcal{W}_1\mathcal{W}_3-\vartheta_2(\phi_1+\phi_2)\phi_2\mathcal{W}_1+\vartheta_2\vartheta_1\phi_2\mathcal{W}_4+\vartheta_2^2\phi_2\mathcal{W}_5\\ -\vartheta_2(\phi_1+\vartheta_2)\phi_2\mathcal{W}_1+\vartheta_2(\phi_1+\vartheta_2)^2\mathcal{W}_5\Big).\end{cases}$$

$$\vdots,$$

$$\mathcal{E}_0(\zeta)=\mathcal{W}_2,$$

$$\mathcal{E}_1(\zeta)=\left[\frac{1-\wp}{\Lambda(\wp)}+\frac{\wp}{\Lambda(\wp)}\frac{\zeta^{\wp}}{\Gamma(\wp+1)}\right]\Big(\lambda\mathcal{W}_1\mathcal{W}_3-(\phi_1+\rho)\mathcal{W}_2\Big),$$

$$\mathcal{E}_2(\zeta)=\frac{1}{(\Lambda(\wp))^2}\left[(1-\wp)^2+\frac{2\wp(1-\wp)(\zeta)^{\wp}}{\Gamma(\wp+1)}+\frac{\wp^2(t^{2\wp})}{\Gamma(2\wp+1)}\right]$$

$$\times\begin{cases}\Big(\Delta\lambda\mathcal{W}_3-\lambda^2\mathcal{W}_1\mathcal{W}_3^2-(\phi_1+\phi_2)\lambda\mathcal{W}_1\mathcal{W}_3+\vartheta_1\lambda\mathcal{W}_3\mathcal{W}_4+\vartheta_2\lambda\mathcal{W}_3\mathcal{W}_5+\rho\lambda\mathcal{W}_1\mathcal{W}_2\\ -(\phi_1+\gamma+\sigma)\lambda\mathcal{W}_1\mathcal{W}_3-(\phi_1+\rho)\lambda\mathcal{W}_1\mathcal{W}_3+(\phi_1+\rho)^2\mathcal{W}_2\Big),\end{cases}$$

$$\mathcal{E}_3(\zeta)=\frac{\Delta\lambda\mathcal{W}_3}{(\Lambda(\wp))^2}\left[(1-\wp)^2+\frac{2\wp(1-\wp)(\zeta)^{\wp}}{\Gamma(\wp+1)}+\frac{\wp^2(\zeta^{2\wp})}{\Gamma(2\wp+1)}\right]$$

$$-\frac{1}{(\Lambda(\wp))^3}\left[(1-\wp)^3+\frac{3\wp(1-\wp)^2(\zeta)^{\wp}}{\Gamma(\wp+1)}+\frac{3\wp^2(1-\wp)(\zeta^{2\wp})}{\Gamma(2\wp+1)}+\frac{\wp^3\zeta^{3\wp}}{\Gamma(3\wp+1)}\right]$$

$$\times\begin{cases}\Big(-\rho\lambda^2\mathcal{W}_1\mathcal{W}_2\mathcal{W}_3+(\phi_1+\gamma+\sigma)\lambda^2\mathcal{W}_1\mathcal{W}_3^2-\Delta\lambda^2\mathcal{W}_3^2+\lambda^3\mathcal{W}_1\mathcal{W}_3^3\\ +(\phi_1+\phi_2)\lambda^2\mathcal{W}_1\mathcal{W}_3^2-\vartheta_1\lambda^2\mathcal{W}_3^2\mathcal{W}_4-\vartheta_2\lambda^2\mathcal{W}_3^2\mathcal{W}_5+\Delta\lambda(\phi_1+\phi_2)\mathcal{W}_3\\ -\lambda^2(\phi_1+\phi_2)\mathcal{W}_1\mathcal{W}_3^2-\lambda(\phi_1+\phi_2)^2\mathcal{W}_1\mathcal{W}_3+\vartheta_1\lambda(\phi_1+\phi_2)\mathcal{W}_3\mathcal{W}_4\\ +\vartheta_2\lambda(\phi_1+\phi_2)\mathcal{W}_3\mathcal{W}_5-\lambda\vartheta_1\sigma\mathcal{W}_3^2+\vartheta_1\lambda(\phi_1+\vartheta_1)\mathcal{W}_3\mathcal{W}_4\\ -\lambda\vartheta_2\phi_2\mathcal{W}_1\mathcal{W}_3+(\phi_1+\vartheta_2)\vartheta_2\lambda\mathcal{W}_3\mathcal{W}_5\Big)\end{cases}$$

$$+\begin{cases}\Big(\Big[\Delta\lambda-\lambda^2\mathcal{W}_1\mathcal{W}_3-\lambda(\phi_1+\phi_2)\mathcal{W}_1+\vartheta_1\lambda\mathcal{W}_4+\vartheta_2\lambda\mathcal{W}_5\Big].\Big[\Delta\lambda\mathcal{W}_2-(\phi_1+\gamma+\sigma)\lambda\mathcal{W}_3\Big]\Big)\\ \quad+\Big(\rho\lambda^2\mathcal{W}_1^2\mathcal{W}_3-(\phi_1+\rho)\rho\lambda\mathcal{W}_1\mathcal{W}_2+(\phi_1+\gamma+\sigma)\rho\lambda\mathcal{W}_1\mathcal{W}_2-(\phi_1+\gamma+\sigma)^2\lambda\mathcal{W}_1\mathcal{W}_3\Big)\end{cases}$$

$$+\begin{cases}\Big((\phi_1+\rho)\rho\lambda\mathcal{W}_1\mathcal{W}_2-\lambda(\phi_1+\rho)(\phi_1+\gamma+\sigma)\mathcal{W}_1\mathcal{W}_3+\Delta\lambda(\phi_1+\rho)\mathcal{W}_3-(\phi_1+\rho)\lambda^2\mathcal{W}_1\mathcal{W}_3^2\\ -(\phi_1+\rho)(\phi_1+\phi_2)\lambda\mathcal{W}_1\mathcal{W}_3+\vartheta_1\lambda(\phi_1+\rho)\mathcal{W}_3\mathcal{W}_4+(\phi_1+\rho)\vartheta_2\lambda\mathcal{W}_3\mathcal{W}_5-(\phi_1+\rho)^2\lambda\mathcal{W}_1\mathcal{W}_3\\ +(\phi_1+\rho)^3\mathcal{W}_2)\Big).\end{cases}$$

$$\vdots,$$

$$\mathcal{I}_0(\zeta)=\mathcal{W}_3,$$

$$\mathcal{I}_1(\zeta)=\left[\frac{1-\wp}{\Lambda(\wp)}+\frac{\wp}{\Lambda(\wp)}\frac{\zeta^{\wp}}{\Gamma(\wp+1)}\right]\Big(\rho\mathcal{W}_2-(\phi_1+\gamma+\sigma_1)\mathcal{W}_3\Big),$$

$$\mathcal{I}_2(\zeta)=\frac{1}{(\Lambda(\wp))^2}\left[(1-\wp)^2+\frac{2\wp(1-\wp)(\zeta)^{\wp}}{\Gamma(\wp+1)}+\frac{\wp^2(\zeta^{2\wp})}{\Gamma(2\wp+1)}\right]$$
$$\Big(\rho\lambda\mathcal{W}_1\mathcal{W}_3-(\phi_1+\rho)\rho\mathcal{W}_2-(\phi_1+\gamma+\sigma)\rho\mathcal{W}_2+(\phi_1+\gamma+\sigma)^2\mathcal{W}_3\Big),$$

$$\mathcal{I}_3(\zeta)=\frac{1}{(\Lambda(\wp))^3}\left[(1-\wp)^3+\frac{3\wp(1-\wp)^2(\zeta)^{\wp}}{\Gamma(\wp+1)}+\frac{3\wp^2(1-\wp)(t^{2\wp})}{\Gamma(2\wp+1)}+\frac{\wp^3\zeta^{3\wp}}{\Gamma(3\wp+1)}\right]$$
$$\times\begin{cases}\Big(\rho^2\lambda\mathcal{W}_1\mathcal{W}_2-\lambda\rho(\phi_1+\gamma+\sigma)\mathcal{W}_1\mathcal{W}_3+\rho\lambda\Delta\mathcal{W}_3-\rho\lambda^2\mathcal{W}_1\mathcal{W}_3^2-\rho(\phi_1+\phi_2)\lambda\mathcal{W}_1\mathcal{W}_3\\ +\vartheta_1\rho\lambda\mathcal{W}_3\mathcal{W}_4+\vartheta_2\rho\lambda\mathcal{W}_3\mathcal{W}_5-(\phi_1+\rho)\rho\lambda\mathcal{W}_1\mathcal{W}_3+\rho(\phi_1+\rho)^2\mathcal{W}_2\\ -(\phi_1+\gamma+\sigma)\rho\lambda\mathcal{W}_1\mathcal{W}_3+(\phi_1+\rho)(\phi_1+\gamma+\sigma)\rho\mathcal{W}_2+(\phi_1+\gamma+\sigma)^2\rho\mathcal{W}_2\\ -(\phi_1+\gamma+\sigma)^3\mathcal{W}_3\Big)\end{cases},$$

$$\vdots,$$

$$\mathcal{R}_0(\zeta)=\mathcal{W}_4,$$

$$\mathcal{R}_1(\zeta)=\left[\frac{1-\wp}{\Lambda(\wp)}+\frac{\wp}{\Lambda(\wp)}\frac{\zeta^{\wp}}{\Gamma(\wp+1)}\right]\Big(\sigma\mathcal{W}_3-(\phi_1+\vartheta_1)\mathcal{W}_4\Big),$$

$$\mathcal{R}_2(\zeta)=\frac{1}{(\Lambda(\wp))^2}\left[(1-\wp)^2+\frac{2\wp(1-\wp)(\zeta)^{\wp}}{\Gamma(\wp+1)}+\frac{\wp^2(\zeta^{2\wp})}{\Gamma(2\wp+1)}\right]$$
$$\Big(\sigma\rho\mathcal{W}_2-\sigma(\phi_1+\gamma+\sigma)\mathcal{W}_3-\sigma(\phi_1+\vartheta_1)\mathcal{W}_3+(\phi_1+\vartheta_1)^2\mathcal{W}_4\Big),$$

$$\mathcal{R}_3(\zeta)=\frac{1}{(\Lambda(\wp))^3}\left[(1-\wp)^3+\frac{3\wp(1-\wp)^2(\zeta)^{\wp}}{\Gamma(\wp+1)}+\frac{3\wp^2(1-\wp)(\zeta^{2\wp})}{\Gamma(2\wp+1)}+\frac{\wp^3\zeta^{3\wp}}{\Gamma(3\wp+1)}\right]$$
$$\times\begin{cases}\Big(\rho\lambda\sigma\mathcal{W}_1\mathcal{W}_3-\rho\sigma(\phi_1+\rho)\mathcal{W}_2-\rho\sigma(\phi_1+\gamma+\sigma)\mathcal{W}_2-\sigma(\phi_1+\gamma+\sigma)^2\mathcal{W}_3\\ -(\phi_1+\vartheta_1)\sigma\rho\mathcal{W}_2+\sigma(\phi_1+\vartheta_1)(\phi_1+\gamma+\sigma)\mathcal{W}_3+\sigma(\phi_1+\vartheta_1)^2\mathcal{W}_3-(\phi_1+\vartheta_1)^3\mathcal{W}_4\Big)\end{cases}$$

$$\vdots,$$

and

$$\mathcal{V}_0(\zeta)=\mathcal{W}_5,$$

$$\mathcal{V}_1(\zeta)=\left[\frac{1-\wp}{\Lambda(\wp)}+\frac{\wp}{\Lambda(\wp)}\frac{\zeta^{\wp}}{\Gamma(\wp+1)}\right]\Big(\phi_2\mathcal{W}_1-(\phi_1+\vartheta_2)\mathcal{W}_5\Big),$$

$$\mathcal{V}_2(\zeta)=\frac{1}{(\Lambda(\wp))^2}\left[(1-\wp)^2+\frac{2\wp(1-\wp)(\zeta)^{\wp}}{\Gamma(\wp+1)}+\frac{\wp^2(\zeta^{2\wp})}{\Gamma(2\wp+1)}\right]$$
$$\times\Big\{\Big(\Delta\phi_2-\lambda\phi_2\mathcal{W}_1\mathcal{W}_3-(\phi_1+\phi_2)\phi_2\mathcal{W}_1+\vartheta_1\phi_2\mathcal{W}_4+\vartheta_2\phi_2\mathcal{W}_5-(\phi_1+\vartheta_2)\phi_2\mathcal{W}_1+(\phi_1+\vartheta_2)^2\mathcal{W}_5\Big),$$

$$\mathcal{V}_3(\zeta)=\frac{\Delta\phi_2}{(\Lambda(\wp))^2}\left[(1-\wp)^2+\frac{2\wp(1-\wp)(\zeta)^{\wp}}{\Gamma(\wp+1)}+\frac{\wp^2(\zeta^{2\wp})}{\Gamma(2\wp+1)}\right]$$
$$-\frac{1}{(\Lambda(\wp))^3}\left[(1-\wp)^3+\frac{3\wp(1-\wp)^2(\zeta)^{\wp}}{\Gamma(\wp+1)}+\frac{3\wp^3(1-\wp)(\zeta^{2\wp})}{\Gamma(2\wp+1)}+\frac{\wp^3\zeta^{3\wp}}{\Gamma(3\wp+1)}\right]$$

Table 2
Description of model's parameters.

$S(\zeta)$	Amount of susceptible Class in time t	100
$\mathcal{E}(\zeta)$	Amount of Exposed Class in time t	3
$\mathcal{I}(\zeta)$	Amount of Infectious Class in time t	1
$\mathcal{R}(\zeta)$	Amount of Recovered Class in time t	0
$\mathcal{V}(\zeta)$	Amount of Vaccinated Class in time t	0
ϕ_1	Crashing rate of the Sensor node	0.003
Δ	inclusion of new sensor nodes	0.33
γ	crashing rate due to attack of worms	0.07
λ	infectivity contact rate	0.1
ρ	rate of transmission from $\mathcal{E}$-class to $\mathcal{I}$-class	Assumed
σ	rate of recovery	Assumed
ϑ_1	rate of transfer from $\mathcal{R}$-class to S-class	Assumed
ϑ_2	rate of transmission from $\mathcal{V}$-class to S-class	Assumed

$$\times\begin{cases}\Big(\rho\lambda\phi_2\mathcal{W}_1\mathcal{W}_2-(\phi_1+\gamma+\sigma)\phi_2\lambda\mathcal{W}_1\mathcal{W}_3+\lambda\Delta\phi_2\mathcal{W}_3-\lambda^2\phi_2\mathcal{W}_1\mathcal{W}_3^2-\lambda\phi_2(\phi_1+\phi_2)\mathcal{W}_1\mathcal{W}_3+\vartheta_1\lambda\phi_2\mathcal{W}_3\mathcal{W}_4\\ +\vartheta_2\lambda\phi_2\mathcal{W}_3\mathcal{W}_5-(\phi_1+\phi_2)\phi_2\Delta+\lambda\phi_2(\phi_1+\phi_2)\mathcal{W}_1\mathcal{W}_3+(\phi_1+\phi_2)^2\phi_2\mathcal{W}_1-\vartheta_1\phi_2(\phi_1+\phi_2)\mathcal{W}_4\\ -\vartheta_2\phi_2(\phi_1+\phi_2)\mathcal{W}_5+\vartheta_1\sigma\phi_2\mathcal{W}_3-\vartheta_1\phi_2(\phi_1+\vartheta_1)\mathcal{W}_4+\phi_2^2\vartheta_2\mathcal{W}_1-\vartheta_2(\phi_1+\vartheta_2)\phi_2\mathcal{W}_5+(\phi_1+\vartheta_2)\Delta\phi_2\\ -\lambda\phi_2(\phi_1+\vartheta_2)\mathcal{W}_1\mathcal{W}_3-(\phi_1+\phi_2)\phi_2(\phi_1+\vartheta_2)\mathcal{W}_1+\phi_2\vartheta_1(\phi_1+\vartheta_2)\mathcal{W}_4+\phi_2\vartheta_2(\phi_1+\vartheta_2)\mathcal{W}_5\\ -(\phi_1+\vartheta_2)^2\phi_2\mathcal{W}_1+(\phi_1+\vartheta_2)^3\phi_2\mathcal{W}_5\Big).\end{cases}$$

5.1. Results and discussion

In what follows, we consider the WP model in WSNs, which is highly valuable because military personnel can deploy WSNs for a variety of tasks, including force defense and insurgent detection in inaccessible regions. Such networks, which have the necessary sensors installed, can identify hostile forces, monitor adversary movements, and analyze the movements and advancements of the opponent.

In this work, we considered the fractional-order WP model in WSNs interms of the HPM which is defined by [30], $\mathcal{ZZ}$ transform [52] has been employed in the frame of ABC fractional derivative operator WSNs is examined. The most significant difference in the present research is the diversity of the HP-$\mathcal{ZZ}$TM and ABC fractional derivative operators. For the sake of comprehensiveness, we go into depth below on the mathematical model for the WP model in WSNs, as it is depicted in Fig. 2. Several system parameters are presented in Table 2. Following that, several numerical simulations have been constructed to characterize the WP model in WSNs. Several of these modeling methodologies for worms are fractional DE simulations, which suggest that treatment time has no impact at all on the rate of recidivism. Applying the ideas of fractional epidemiology [57,58], we established a fractional-order WP in the WSNs model method for this study that consisted of control symptoms. The strategy accounts for the chance of recurrence, which fluctuates based on the overall duration of the infectious treatment. Fig. 3 (**a**-**e**) represents the dynamical behavior of the system under different parametric values. In Fig. 3 (**a**-**e**), a strong effect of immunization $\mathcal{V}$ given to the sensor nodes appears over the revealed $\mathcal{E}$ and infectious class $\mathcal{I}$, respectively. It is noted that while fewer detectors will transmit messages to fusion labs when only a handful of detectors are encompassed by a specific node arrangement, the ensuing power use will also be minimal with the reduction in fractional-order $\wp = 0.75$. Thus, when deploying nodes that have restricted broadcast dominance, our main objective is to concurrently boost connectivity and decrease power usage if $\wp = 1$.

In Fig. 4 (**a**-**e**), for every $\rho = 0.28$ node in every stage of a homogeneous WSN that has identical properties, factor ρ is constant and has no bearing on improvement. The diversity of access points in a diverse WSN, however, results in networks with varying transmitter strengths with fractional-order $\wp = 1$ has sensitivity criteria; as a result, the value of fractional-order will depend on each node's value.

In higher values of ϑ_1, a suitable node positioning attempts to reduce $\mathcal{E}$ when $\wp = 0.75$, whereas an ideal setup attempts to decrease $\mathcal{I}$ since detector generation serves disproportionately to the two access point power consumption for minimal values of ϑ_1 compared to access point capacity does, as shown in Fig. 5 (**a**-**e**). It concludes that relocating connections in the direction of the confluence cores will typically enhance the normal spacing between detectors as well as access indications, increasing sensor accuracy.

Fig. 6 (**a**-**e**) shows that the access points' ranges from the fusion nodes typically expand when they are moved closer to the symmetrical gravity centers of the relevant locations with $\vartheta_2 = 0.06$, which raises the accessibility nodes' potency if fractional-order reduces to $\wp = 1$ for the recovered class $\mathcal{R}$. The accessibility point-sensor strength efficiency drops as ϑ_2 grows, as seen in Fig. 6 (**a**-**e**).

Our approach operates better with regard to HP-$\mathcal{ZZ}$TM and ABC techniques of overall transmission and use of power than connections. The suggested algorithm performs poorly even if it uses a lower value ($\sigma = 0.4$) since numerous sensory sites are not within the neighboring connection nodes' transmission capability. Lastly, in contrast to our technique, $\mathcal{S}$ produces a 3% reduction in power consumption but a far less comprehensive fractional-order value $\wp = 0.85$ for $\mathcal{V}$. The figure indicates that the recovery is quite substantial when appropriate parameters are included in Fig. 7 (**a**-**e**).

For $\vartheta_1 = 0.3$, the illustration shows that the rate of recovery $\mathcal{R}$ is fairly substantial when suitable factors are considered and critical nodes in the network are discouraged from engaging in a multicasting task. Fig. 8 (**a**-**e**) shows the transformation of the recovering group of networks to the susceptibility group of nodes, while $\mathcal{I}$ shows the changing dynamics of the immunized group of nodes vs. the

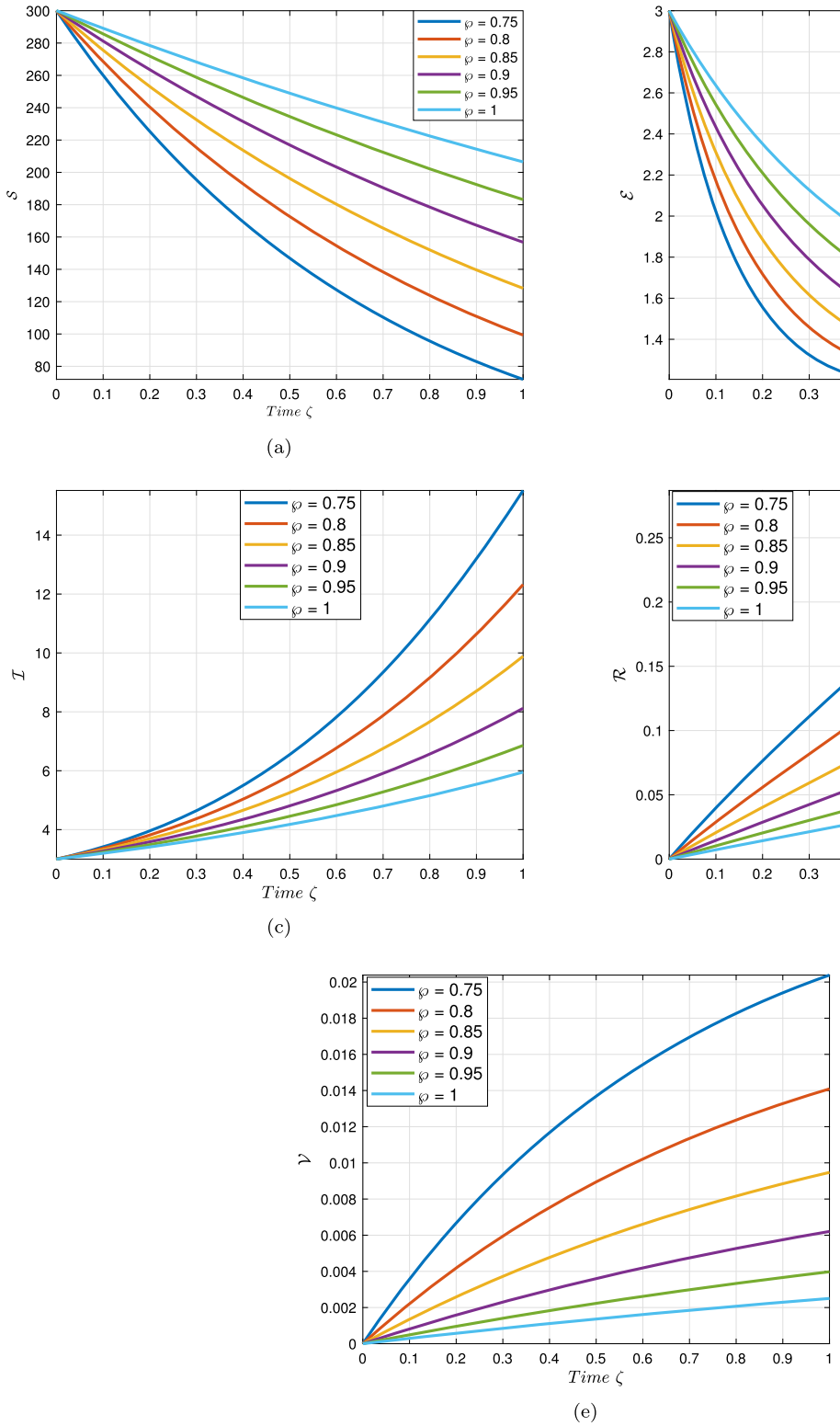

Fig. 3. Two dimensional illustrations for WP model in the WSNs (3.2) for various fractional-order and $\sigma = 0.45$.

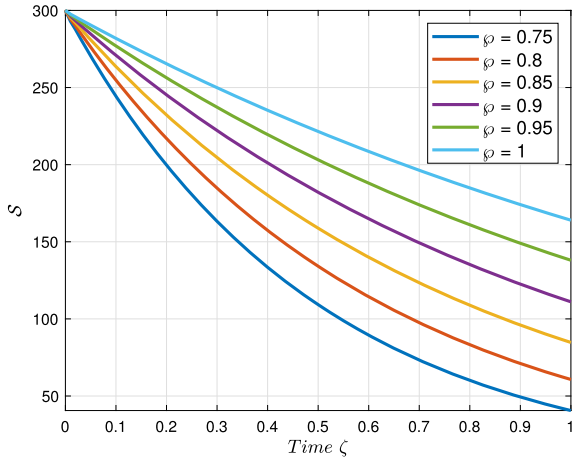

(a)

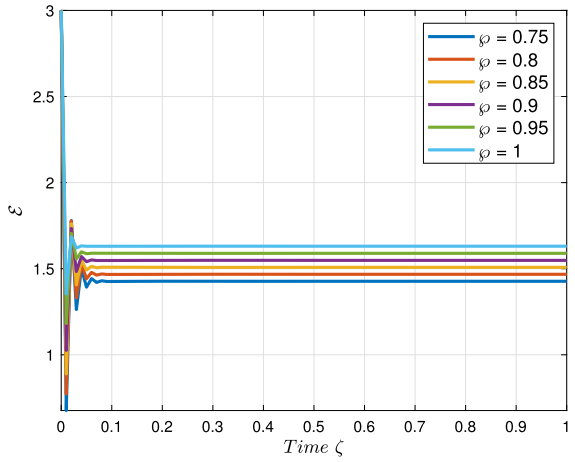

(b)

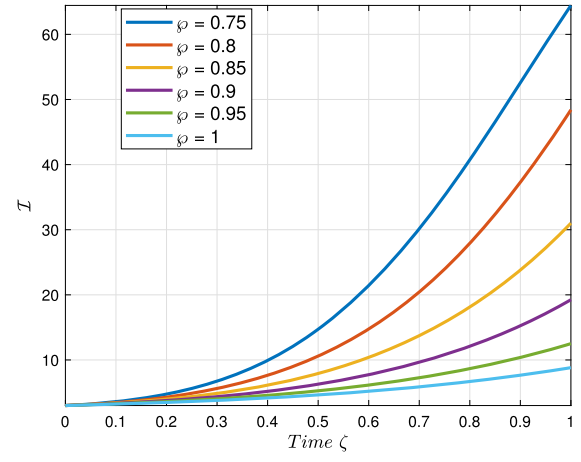

(c)

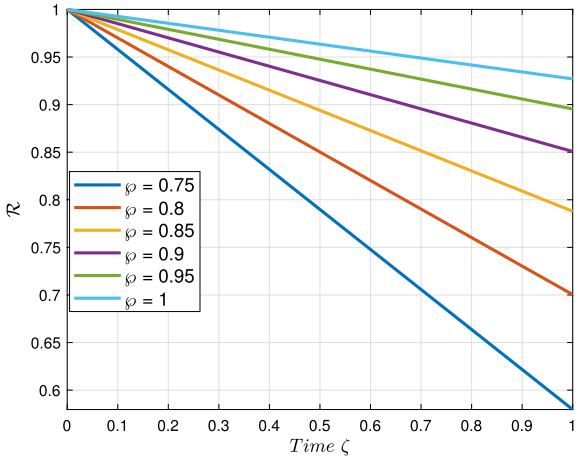

(d)

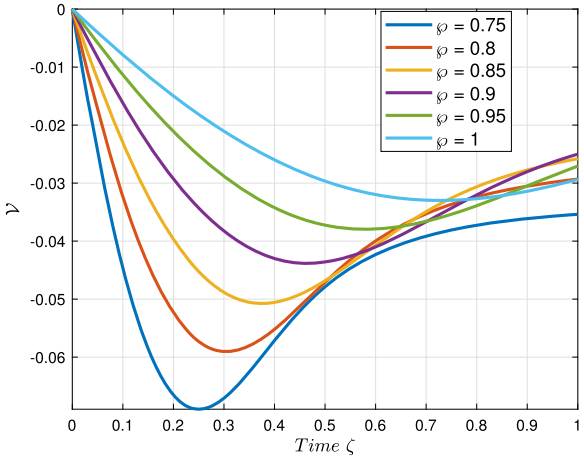

(e)

Fig. 4. Two dimensional illustrations for WP model in the WSNs (3.2) for various fractional-order and $\rho = 0.28$.

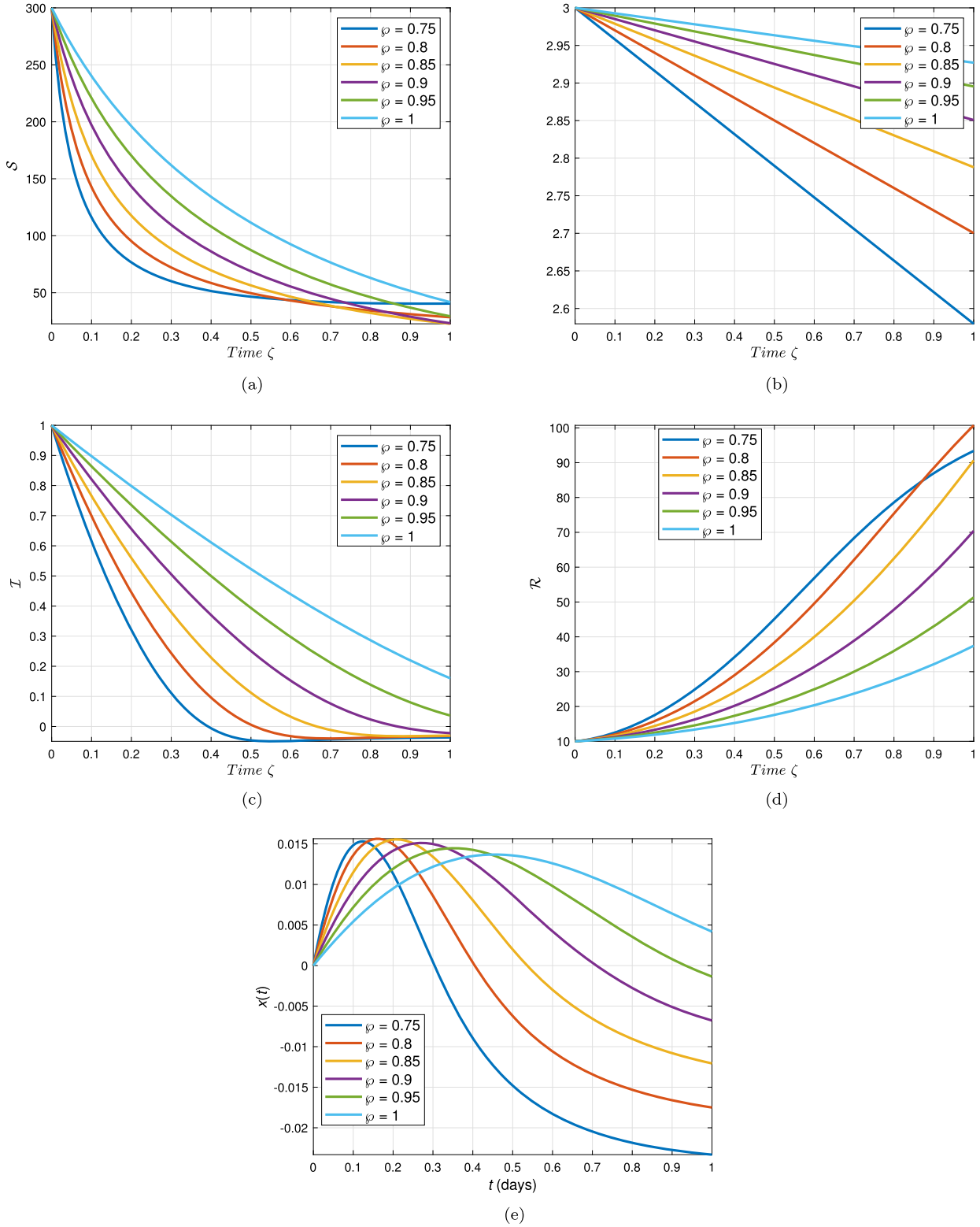

Fig. 5. Two dimensional illustrations for WP model in the WSNs (3.2) for various fractional-order and $\vartheta_1 = 0.39$.

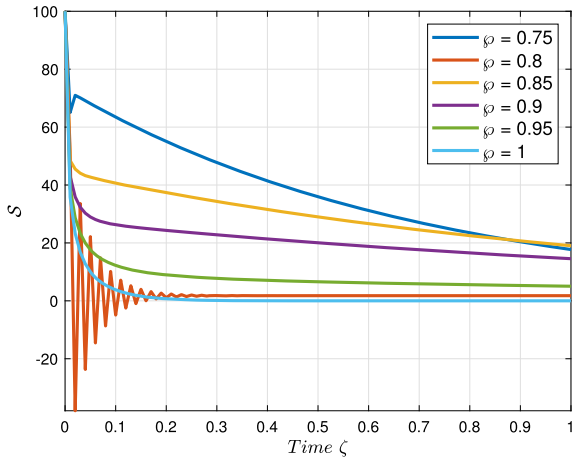

(a)

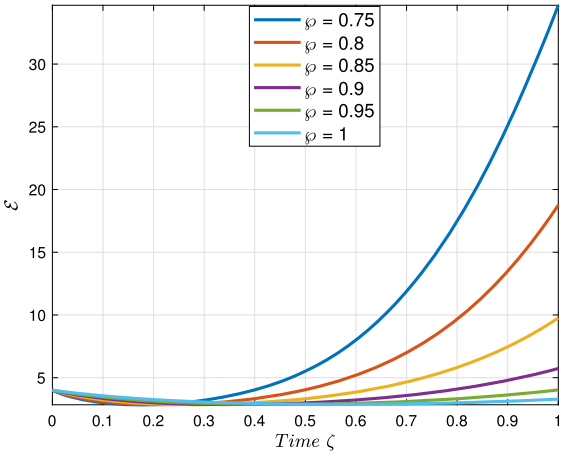

(b)

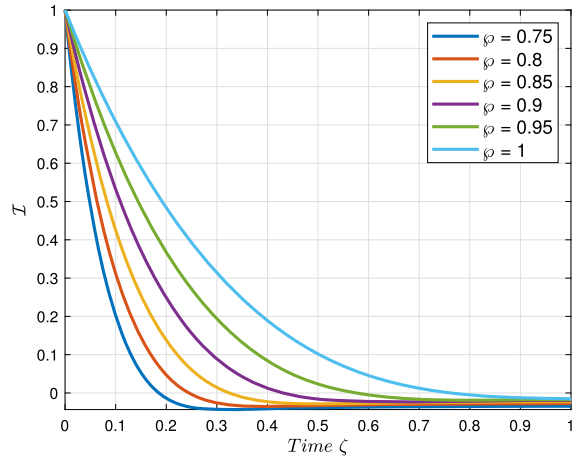

(c)

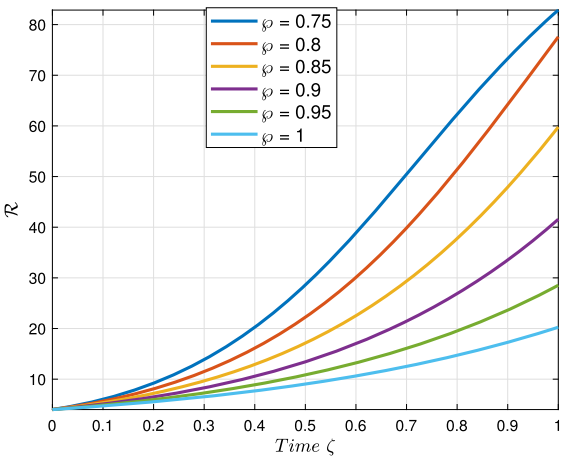

(d)

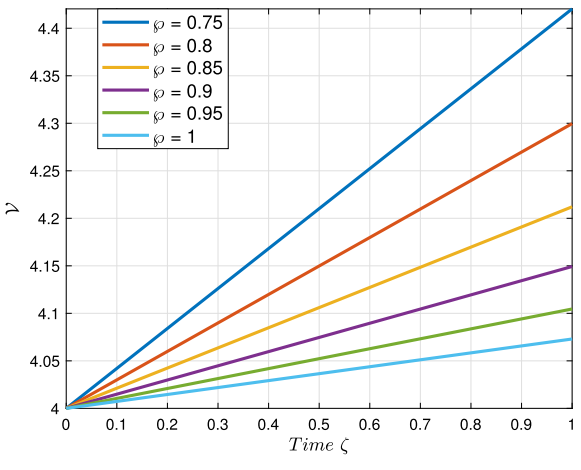

(e)

Fig. 6. Two dimensional illustrations for WP model in the WSNs (3.2) for various fractional-order and $\vartheta_2 = 0.06$.

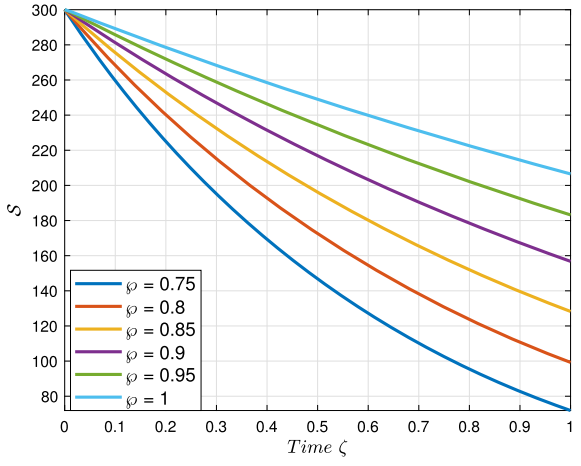

(a)

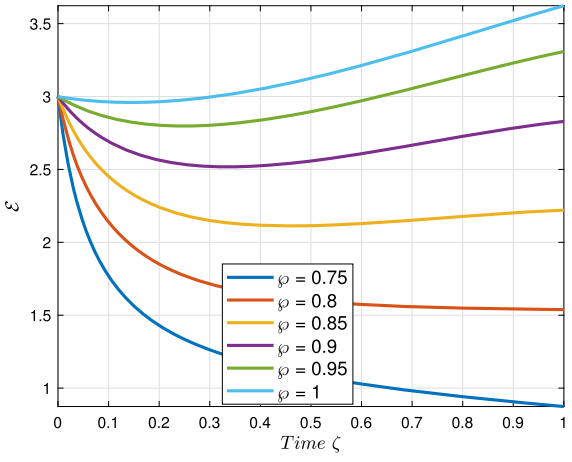

(b)

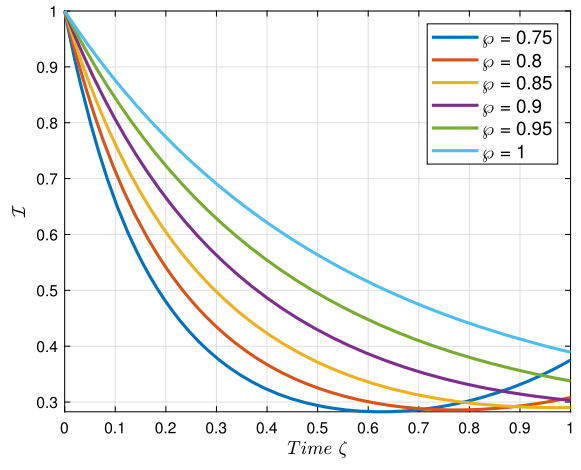

(c)

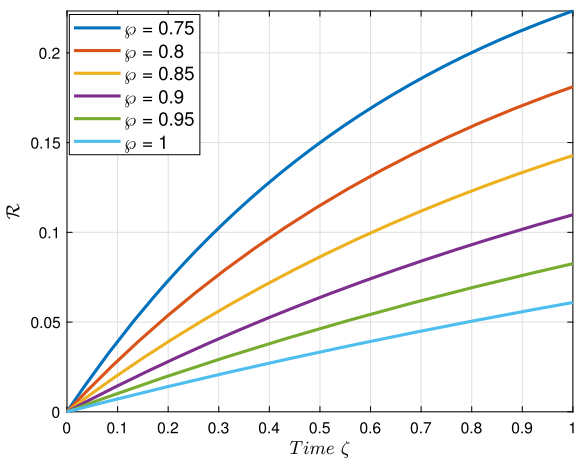

(d)

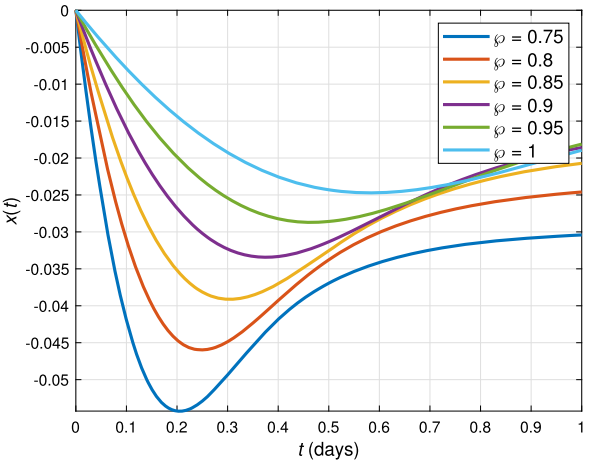

(e)

Fig. 7. Two dimensional illustrations for WP model in the WSNs (3.2) for various fractional-order and $\sigma = 0.4$.

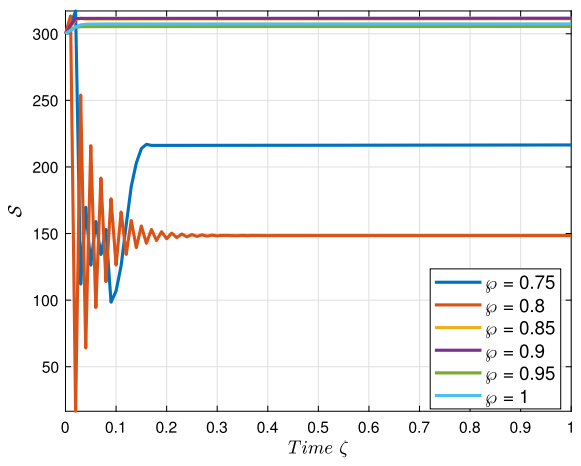

(a)

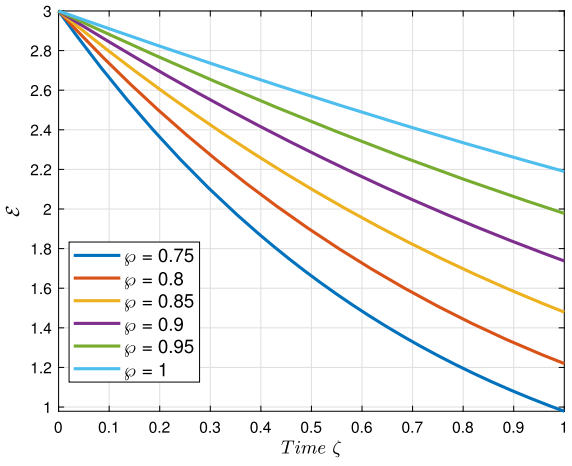

(b)

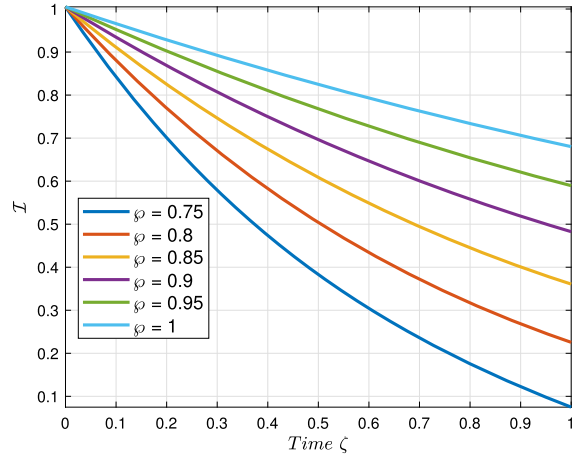

(c)

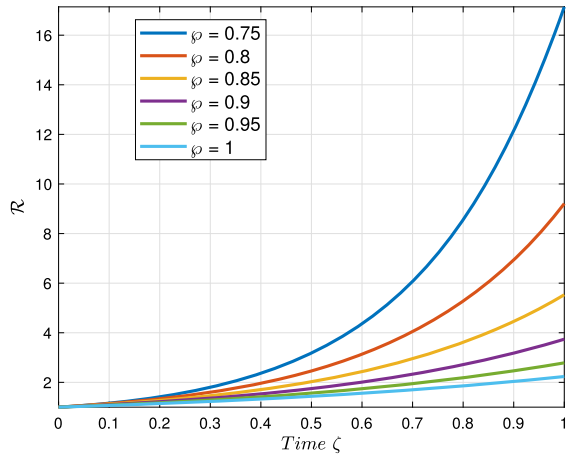

(d)

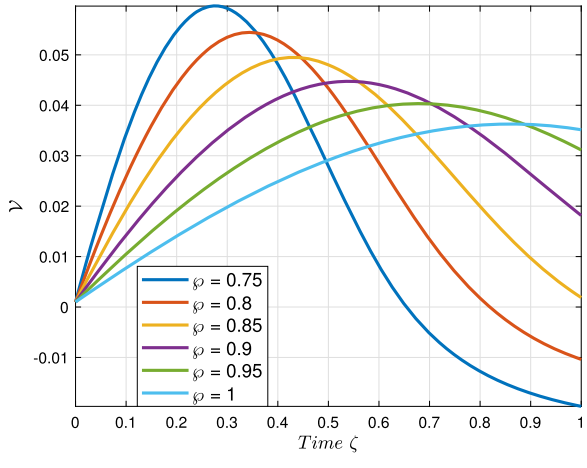

(e)

Fig. 8. Two dimensional illustrations for WP model in the WSNs (3.2) for various fractional-order and $\vartheta_1 = 0.30$.

susceptibility group of clusters when fractional-order fluctuations from $\wp = 0.75$ to $\wp = 1$, respectively. The likelihood of a malware assault on sensors will be minimal if they receive the appropriate vaccination.

In a nutshell, this research will help the software company produce antivirus software that is incredibly effective in reducing the number of harmful signals that may impact sensor nodes. Additionally, the study should offer end users recommendations on how to vaccinate properly and consistently employ antivirus software on sensor nodes in the area of sensors in order to strengthen defences against attacks. Our new HP-$\mathcal{ZZ}$TM algorithm guarantees every connection is effective, even in situations where the communication bandwidth is restricted. According to simulation findings, our strategies outperform others in terms of fractional calculus approach, network accessibility, and consumed power.

6. The $0-1$ test and complexity analysis

This section examines the broad spectrum of chaos practices to assess the fascinating aspects of chaotic processes, wherein the more sophisticated the framework, the more chaotic it gets. The problems of this proposed WP model (3.2) are now evaluated by means of the $\mathbb{C}_0$ complexity approach and the approximation efficiency (ApEn) analysis. Furthermore, to confirm the presence of randomness in the WP model (3.2), the $0-1$ technique will be employed.

6.1. The $0-1$ test

The purpose of this part is to demonstrate the $0-1$ assessment, a theory put forth by Gottwald and Melbourne [59], regularly to operate multifaceted structures and make distinctions inside chaos. We consider the statistical trend as reinforcement; in the case where the construction of the system is chaotic, the estimated number is close to 1; in the other case, it will be close to 0. Furthermore, we depict the process as follows: First, we use time-domain research to find the transforming components shown below: $(\mathbf{v}(\Bbbk))_{\Bbbk=1,\ldots,\tilde{\mathcal{N}}}$:

$$\mathbf{w}_{\Upsilon}(\upsilon)=\sum_{\Bbbk=1}^{\upsilon}\mathbf{v}(\Bbbk)\cos(\imath\Upsilon),\quad \tilde{\mathbf{w}}_{\Upsilon}(\upsilon)=\sum_{\Bbbk=1}^{\upsilon}\mathbf{v}(\Bbbk)\sin(\imath\Upsilon),\quad \upsilon=1,2,\ldots,\tilde{\mathcal{N}}.$$

Using the $(\mathbf{w}_{\Upsilon}-\tilde{\mathbf{w}}_{\Upsilon})$ plot, one can ascertain how much chaos behavior is present in the proposed WP structure. The design of the experiment is periodic if the trajectory parameters of $\mathbf{w}_{\Upsilon}$ and $\tilde{\mathbf{w}}_{\Upsilon}$ are constrained; the connections within the context become chaotic anytime the experiment performs such a Brownian motion. Furthermore, the mean square displacement expression is presented below:

$$F_{\Upsilon}(\upsilon)=\frac{1}{\tilde{\mathcal{N}}}\sum_{\Bbbk=1}^{\tilde{\mathcal{N}}}\left\{\left(\mathbf{w}_{\Upsilon}(\Bbbk+\upsilon)-\mathbf{w}_{\Upsilon}(\Bbbk)\right)^2+\left(\tilde{\mathbf{w}}_{\Upsilon}(\Bbbk+\upsilon)-\tilde{\mathbf{w}}_{\Upsilon}(\Bbbk)\right)^2\right\},\quad \tilde{\mathcal{N}}\geq 10\upsilon.$$

Moreover, we show the following autonomous growth:

$$\Theta_{\Upsilon}=\lim_{\upsilon\mapsto\infty}\frac{\log F_{\Upsilon}}{\log\upsilon}.$$

The growth rate "$\Theta = median(\Theta_{\Upsilon})$" in the broader setting of the given WP model (3.2) allows to distinguish both non-chaotic and chaotic behavior. The model is chaotic when Θ is next to 1, but it is not chaotic when Θ equates to 0.

The autonomous exponential rate of progression Θ of the corresponding fractional WP model (3.2) for $\wp \in (0,1]$, where $\vartheta_1 = 0.30$ and $\sigma = 0.4$, respectively, is shown in Fig. 9. Anyone understands that the growth rate Θ discusses one whereas the value of ϑ_1 decreases. It suggests that the corresponding fractional WP model (3.2) displays chaotic consequences. Fig. 9 ((a)-(c)) illustrates the results of the $\mathbf{w}_{\Upsilon}-\tilde{\mathbf{w}}_{\Upsilon}$ schematics for different fractional data and settings, respectively, demonstrating that there is disorder in the fractional WP model (3.2). It is evident from Figs. 9((d)-(f)) that this system is oscillating because of the sharply limited channels. Conversely, Brownian-like paths are shown in Fig. 9, indicating the existence of in chaotic actions in the fractional WP system (3.2).

6.2. The ApEn of the proposed model

At the moment, we use the approximation entropy (ApEn) method [60] to characterize the complex configuration of the fractional WP model (3.2). An indication of the complexity of time-dependent series-generated systems is the ApEn. It needs to be mentioned that evidence sources with higher ApEn values have more perspectives. The first $\mathbf{p}-\Bbbk+1$ accessible patterns are identified below in order to determine ApEn:

$$\mathcal{U}(\imath)=\left[\mathbf{v}(\imath),\ldots,\mathbf{v}(\imath+\Bbbk-1)\right],\quad \forall\,\imath\in[\imath+\Bbbk-1],$$

where $\mathbf{v}(1),\mathbf{v}(2),\ldots,\mathbf{v}(\mathbf{p})$ is an array of isolated objects. Additionally, we use the procedure to characterize each part $\mathbb{C}_{\imath}^{\Bbbk}(\mathbf{r})=\Theta/(\mathbf{p}-\Bbbk+1)$, where Θ is the dimension of $\mathcal{U}(\imath)$ having $d(\mathcal{U}(\imath),\mathcal{U}(\Bbbk))\leq\mathbf{r}$. Observe that two crucial elements influence the ApEn: the incorporated observations $\Bbbk$ and the appropriate evaluation $\mathbf{r}$. Here, we use $\Bbbk=2$. In $\mathbf{r}=0.3S.D(\mathcal{U})$, $S.D(\mathcal{U})$ is the value of dispersion of the information $\mathcal{U}$, expressed as a positive square root. Thus, the ApEn is as follows:

$$ApEn=\hbar^{\Bbbk}(\mathbf{r})-\hbar^{\Bbbk+1}(\ell),$$

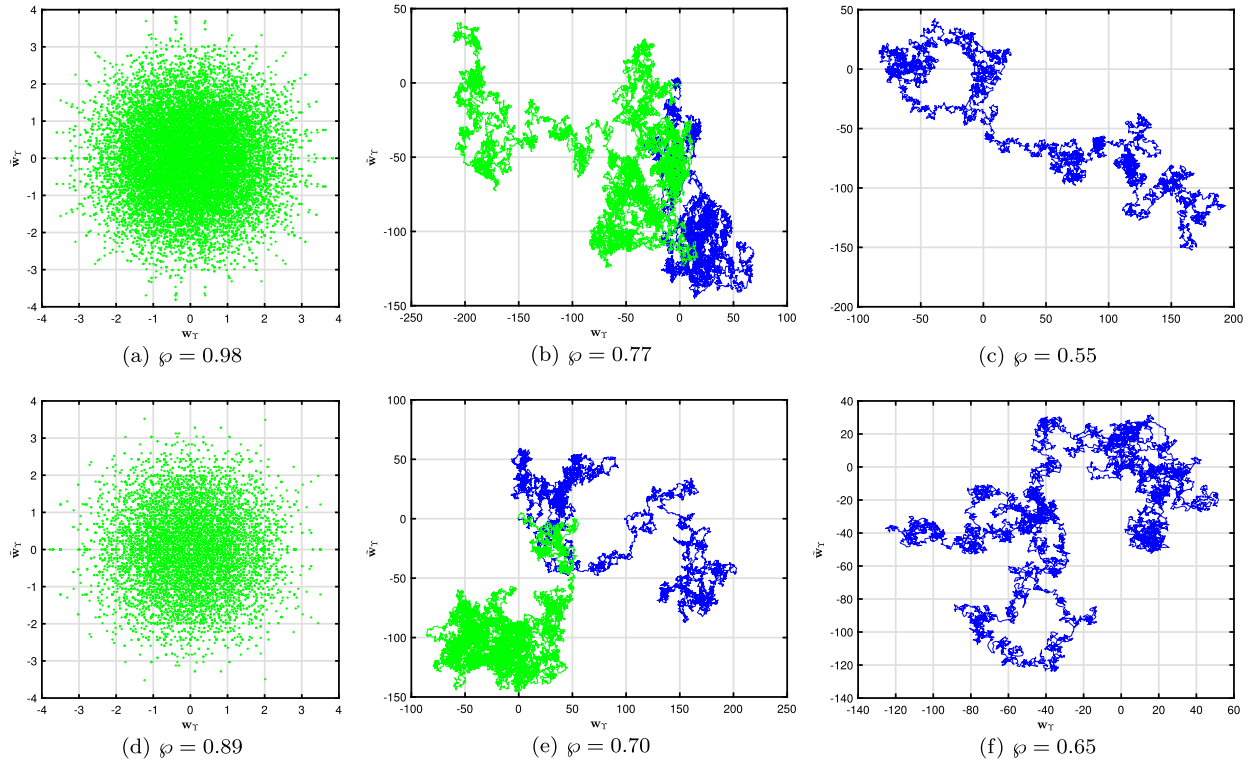

Fig. 9. $\mathbf{w}_\Upsilon - \tilde{\mathbf{w}}_\Upsilon$ depictions of the fractional WP model (3.2) for various values of $\wp$.

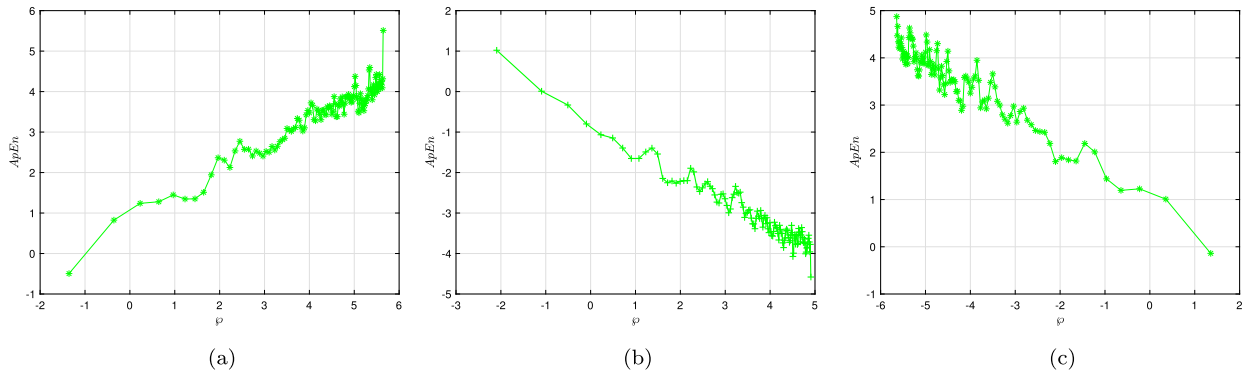

Fig. 10. Graphs for the $\mathbb{C}_0$ of the fractional WP model (3.2) via the system settings mentioned in Table 2 and fractional-order $\wp = 0.96,\ 0.89$ and 0.70.

where

$$\hbar^{\mathbb{k}}(\mathbf{r}) = \frac{1}{\mathbf{p} - \mathbb{k} - 1} \sum_{\iota=0}^{\mathbf{p}-\mathbb{k}+1} \log \mathbb{C}_\iota^{\mathbb{k}}(\mathbf{r}).$$

Selecting the ICs mentioned in Table 2 and the model's settings, $\vartheta_1 = 0.30$ and $\sigma = 0.4$, Figs. 10 (**a-c**) depicts the ApEn corresponds to the fractional WP model (3.2). It seems evident that an advanced phase pattern is required to achieve higher ApEn. These findings thus confirm the existence of chaos in the proposed fractional strategy and align with whichever fractional consequences have been earlier shown.

6.3. The $\mathbb{C}_0$ complexity analysis

In the following, we use the $\mathbb{C}_0$ complexity approach with the inverse Fourier transform (FT) to compute the operational hardness of the suggested WP model (3.2). Here is a detailed description of the process [61].

The following describes the process for calculating the $\mathbb{C}_0$ intricacy throughout a sequence of $\hbar(0), ..., \hbar(\digamma - 1)$:

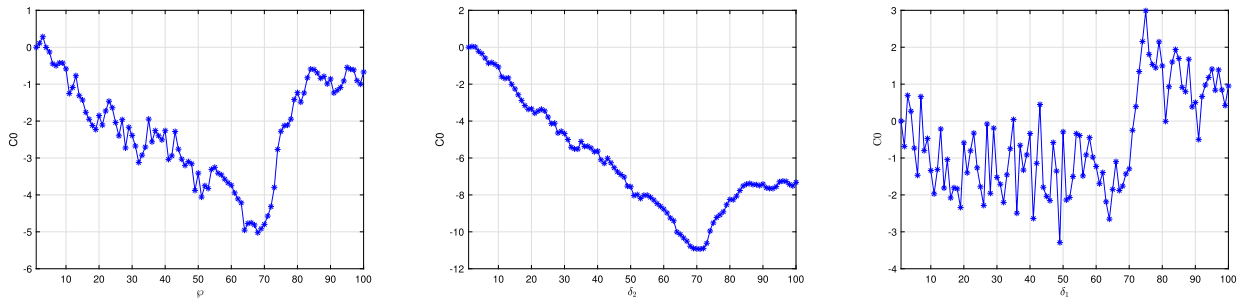

Fig. 11. Graphs for the $\mathbb{C}_0$ of the fractional WP model (3.2) via the system settings mentioned in Table 2 and fractional-order $\wp = 0.96,\ 0.89$ and 0.70.

Step 1: To determine the expression's FT $\mathbf{y}(\mathbb{k})$ as:

$$\mathcal{U}_{\tilde{\mathcal{N}}}(\mathbf{t}) = \frac{1}{\tilde{\mathcal{N}}} \sum_{\eta=0}^{\tilde{\mathcal{N}}-1} \mathbf{y}(\eta) \exp\Big(-2\pi\iota\big(\frac{\upsilon\mathbb{k}}{\mathbf{p}}\big)\Big), \quad \eta = 0, 1, ..., \tilde{\mathcal{N}} - 1.$$

Step 2: This formula yields the mean square:

$$\mathbf{V}_{\tilde{\mathcal{N}}} = \frac{1}{\tilde{\mathcal{N}}} \sum_{\eta=0}^{\tilde{\mathcal{N}}-1} |\mathcal{U}_{\tilde{\mathcal{N}}}(\eta)|^2,$$

where

$$\tilde{\mathcal{U}}_{\tilde{\mathcal{N}}}(\eta) = \begin{cases} \mathcal{U}_{\tilde{\mathcal{N}}}(\eta) & if \quad \|\mathcal{U}_{\tilde{\mathcal{N}}}(\eta)\|^2 > \mathbf{r}\mathbf{V}_{\tilde{\mathcal{N}}}, \\ 0 & if \quad \|\mathcal{U}_{\tilde{\mathcal{N}}}(\eta)\|^2 \le \mathbf{r}\mathbf{V}_{\tilde{\mathcal{N}}}. \end{cases}$$

Step 3: The following method is used for determining the inverse FT:

$$\zeta(\mathbf{t}) = \frac{1}{\tilde{\mathcal{N}}} \sum_{\eta=0}^{\tilde{\mathcal{N}}-1} \tilde{\mathcal{U}}_{\tilde{\mathcal{N}}}(\eta) \exp\Big(-2\pi\iota\big(\frac{\upsilon\mathbb{k}}{\mathbf{p}}\big)\Big), \quad \eta = 0, 1, ..., \tilde{\mathcal{N}} - 1.$$

Step 4: The following process is implemented to determine the extent of $\mathbb{C}_0$:

$$\mathbb{C}_0 = \frac{1}{\sum_{\iota=0}^{\tilde{\mathcal{N}}} \|\mathbf{y}(\iota)\|^2} \sum_{\iota=0}^{\tilde{\mathcal{N}}} \|\zeta(\iota) - \mathbf{y}(\iota)\|$$

Fig. 11 (**a**) illustrates the $\mathbb{C}_0$ intricacy of the fractional WP (3.2) for exhibiting the results of $\mathbb{C}_0$ concerns of the proposed model (3.2). The fractional WP (3.2) exhibits an improvement in $\mathbb{C}_0$ measurements, as seen by Fig. 11 (**b**), in tandem with a reduction in $\sigma = 0.4$. In addition, the spectrum where the situation σ decreases indicates the more significant challenges of the fractional WP framework (3.2) (see Fig. 11 (**c**)). Consequently, the $\mathbb{C}_0$ complexity analysis is a useful tool for quickly determining intricacy.

7. Conclusion

This article constitutes an analysis that explores the characteristics of the $\mathcal{ZZ}$ transform as they relate to the ABC fractional operator. Furthermore, we developed a new road map that is based on the $\mathcal{ZZ}$ transform, the HPM, and the ABC fractional derivative operator. With the aid of the aforesaid technique, we have established the analytical solutions for the nonlinear WP in the WSNs. Consequently, this novel technique has been easy to use and yields the necessary outcomes for the proposed model. Several qualitative aspects of the WP in the WSN model have been investigated in detail. It is concluded that the total number of immunized people increased compared to the results generated via the projected technique. The HP-$\mathcal{ZZ}$TM demonstrated its efficiency and potential for dealing with nonlinearities in the proposed model and allowed us to get an exact solution more quickly with the help of He's polynomials. The HP-$\mathcal{ZZ}$TM is a more vigorous and pragmatic scheme than conventional methods like the Adomian decomposition method and the new iterative transform method.

Moreover, the $0-1$ test has been presented, along with a review analysis using the ApEn methodology and the complexity measure. The complex analysis results show that, although the fractional data is distinctive because the fractional pattern produces an unpredictable approach coupled with a higher degree of difficulty and a wider range of chaotic areas than the classical case.

Several graphical representations have shown that when the fractional-order is reduced to 1, our findings are close to the actual results. This shows that even if two terms from the series solution were taken into consideration, the suggested model still offered

sufficient accuracy for solving the issue. The presented technique has a lesser computational difficulty than the previous numerical procedures. In addition, the method governs and evaluates a series of solutions that quickly approach the precise answer within a brief admissible domain. Due to the noise-free nature of the results, we may avoid the need for rectifying functions, stationary restrictions, or excessive integrals in this approach, which overcomes the limitations of previous methods. Moreover, we anticipate that our method will be utilized in dealing with additional highly complicated non-linear coupled fractional-order equations. We will employ the generalized Kudryashov approach and the double $\mathcal{ZZ}$ transform to examine an analogous issue in future research. This proves to be an advantageous method to address complex phenomena.

Funding statement

This research has no external funding.

CRediT authorship contribution statement

Saima Rashid: Formal analysis, Data curation, Conceptualization. **Rafia Shafique:** Project administration, Methodology, Investigation. **Saima Akram:** Writing – original draft, Visualization, Validation. **Sayed K. Elagan:** Supervision, Methodology, Funding acquisition.

Declaration of competing interest

Authors declare that there are no conflicts of interest.

Data availability

All datasets used to analyze this investigation are freely available from the corresponding author upon reasonable request.

Acknowledgement

The authors extend their appreciation to Taif University, Saudi Arabia, for supporting this work through project number (TU-DSPP-2024-127).

References

[1] E. Altman, T. Basar, T. Jimenez, N. Shimkin, Competitive routing in networks with polynomial costs, IEEE Trans. Autom. Control 47 (1) (2002) 92–96.
[2] E.K. Burke, G. Kendall, Search Methodologies: Introductory Tutorials in Optimization and Decision Support Techniques, Springer, 2014.
[3] N.R. Swamy, Control Algorithms for Networked Control and Communication Systems, The University of Texas at Arlington, 2003.
[4] N.K. Dixit, L. Mishra, M.S. Charan, B.K. Dey, The new age of computer virus and their detection, Int. J. Netw. Secur. Appl. 4 (3) (2012) 79.
[5] B.K. Mishra, D.K. Saini, SEIRS epidemic model with delay for transmission of malicious objects in computer network, Appl. Math. Comput. 188 (2) (2007) 1476–1482.
[6] W.O. Kermack, A.G. McKendrick, A contribution to the mathematical theory of epidemics, Proc. R. Soc. Lond. Ser. A, Contain. Pap. Math. Phys. Character 115 (772) (1927) 700–721.
[7] B.K. Mishra, S.K. Pandey, Dynamic model of worms with vertical transmission in computer network, Appl. Math. Comput. 217 (21) (2011) 8438–8446.
[8] M.E. Newman, S. Forrest, J. Balthrop, Email networks and the spread of computer viruses, Phys. Rev. E 66 (3) (2002) 035101.
[9] M. Draief, A. Ganesh, L. Massoulié, Thresholds for virus spread on networks, in: Proceedings of the 1st International Conference on Performance Evaluation Methodolgies and Tools, VALUETOOLS 2006, Pisa, Italy, October 11-13, 2006, 2006, p. 51-es.
[10] P. Yan, S. Liu, SEIR epidemic model with delay, ANZIAM J. 48 (1) (2006) 119–134.
[11] B.K. Mishra, N. Jha, Fixed period of temporary immunity after run of anti-malicious software on computer nodes, Appl. Math. Comput. 190 (2) (2007) 1207–1212.
[12] J.L. Sanders, Quantitative guidelines for communicable disease control programs, Biometrics (1971) 883–893.
[13] A. Khelil, C. Becker, J. Tian, K. Rothermel, Directed-graph epidemiological models of computer viruses, in: Proc. 5th ACM Int'l Workshop on Modeling Analysis and Simulation of Wireless and Mobile Systems, Proceedings. 1991 IEEE Computer Society Symposium on Research in Security and Privacy, Oakland, CA, USA, 2002, pp. 54–60.
[14] D. Kumar, J. Singh, D. Baleanu, Analysis of regularized long-wave equation associated with a new fractional operator with Mittag-Leffler type kernel, Phys. A, Stat. Mech. Appl. 492 (2018) 155–167.
[15] F. Jarad, T. Abdeljawad, Z. Hammouch, On a class of ordinary differential equations in the frame of Atangana–Baleanu fractional derivative, Chaos Solitons Fractals 117 (2018) 16–20.
[16] T. Abdeljawad, D. Baleanu, Integration by parts and its applications of a new nonlocal fractional derivative with Mittag-Leffler nonsingular kernel, J. Nonlinear Sci. Appl. 10 (2017) 1098–1107.
[17] T. Abdeljawad, D. Baleanu, Discrete fractional differences with nonsingular discrete Mittag-Leffler kernels, Adv. Differ. Equ. 2016 (2016) 1–18.
[18] A. Atangana, D. Baleanu, New fractional derivatives with nonlocal and non-singular kernel: theory and application to heat transfer model, Therm. Sci. 20 (2016).
[19] F. Özköse, M. Yavuz, M.T. Senel, R. Habbireeh, Fractional order modelling of omicron SARS-CoV-2 variant containing heart attack effect using real data from the United Kingdom, Chaos Solitons Fractals 157 (2022) 111954.
[20] M.A. Khan, S. Ullah, S. Kumar, A robust study on 2019-nCOV outbreaks through non-singular derivative, Eur. Phys. J. Plus 136 (2021) 168, https://doi.org/10.1140/epjp/s13360-021-01159-8.
[21] S. Kumar, A. Kumar, B. Samet, H. Dutta, A study on fractional host-parasitoid population dynamical model to describe insect species, Numer. Methods Partial Differ. Equ. 2 (2020).
[22] M. Chinnamuniyandi, S. Chandran, C. Xu, Fractional order uncertain BAM neural networks with mixed time delays: an existence and quasi-uniform stability analysis, J. Intell. Fuzzy Syst. 46 (1) (2024) 1–23, https://doi.org/10.3233/JIFS-234744.

[23] C. Xu, D. Mu, Z. Liu, Y. Pang, M. Liao, C. Aouiti, New insight into bifurcation of fractional-order 4D neural networks incorporating two different time delays, Commun. Nonlinear Sci. Numer. Simul. 118 (2023) 107043.
[24] S. Kumar, R.P. Chauhan, S. Momani, S. Hadid, Numerical investigations on COVID-19 model through singular and non-singular fractional operators, Numer. Methods Partial Differ. Equ. 40 (1) (2024) e22707.
[25] B. Ghanbari, S. Kumar, A study on fractional predator–prey–pathogen model with Mittag–Leffler kernel-based operators, Numer. Methods Partial Differ. Equ. 40 (1) (2024) 22689.
[26] S. Kumar, R. Kumar, S. Momani, S. Hadid, A study on fractional COVID-19 disease model by using Hermite wavelets, Math. Methods Appl. Sci. 46 (7) (2023) 7671–7687.
[27] P. Veeresha, D.G. Prakasha, S. Kumar, A fractional model for propagation of classical optical solitons by using nonsingular derivative, Math. Methods Appl. Sci. (2020).
[28] C. Xu, L. Jinting, Z. Yingyan, C. Qingyi, O. Wei, P. Yicheng, L. Zixin, L. Maoxin, L. Peiluan, New results on bifurcation for fractional-order octonion-valued neural networks involving delays, Netw. Comput. Neural Syst. (2024) 1–53, https://doi.org/10.1080/0954898X.2024.2332662.
[29] C. Xu, M. Farman, A. Shehzad, Analysis and chaotic behavior of a fish farming model with singular and non-singular kernel, Int. J. Biomath. (2023), https://doi.org/10.1142/S179352452350105X.
[30] J.H. He, A coupling method of a homotopy technique and a perturbation technique for non-linear problems, Int. J. Non-Linear Mech. 35 (1) (2000) 37–43.
[31] J.S. Duan, R. Rach, D. Baleanu, A.M. Wazwaz, A review of the Adomian decomposition method and its applications to fractional differential equations, Commun. Fract. Calc. 3 (2) (2012) 73–99.
[32] K. Wang, S. Liu, Application of new iterative transform method and modified fractional homotopy analysis transform method for fractional Fornberg-Whitham equation, J. Nonlinear Sci. Appl. 9 (5) (2016) 2419–2433.
[33] H. Liu, J. Li, Q. Zhang, Lie symmetry analysis and exact explicit solutions for general Burgers' equation, J. Comput. Appl. Math. 228 (1) (2009) 1–9.
[34] O.A. Arqub, M. Al-Smadi, N. Shawagfeh, Solving Fredholm integro–differential equations using reproducing kernel Hilbert space method, Appl. Math. Comput. 219 (17) (2013) 8938–8948.
[35] C. Huang, Z. Zhang, The spectral collocation method for stochastic differential equations, Discrete Contin. Dyn. Syst., Ser. B 18 (3) (2013) 667–679.
[36] T.E. Aravindan, R. Seshasayanan, Denoising brain images with the aid of discrete wavelet transform and monarch butterfly optimization with different noises, J. Med. Syst. 42 (2018) 1–13.
[37] M.M. Khader, K.M. Saad, A numerical approach for solving the fractional Fisher equation using Chebyshev spectral collocation method, Chaos Solitons Fractals 110 (2018) 169–177.
[38] T.N. Narasimhan, Fourier's heat conduction equation: history, influence, and connections, Rev. Geophys. 37 (1) (1999) 151–172.
[39] I. Singh, N.H. Ansari, G. Singh, Solving PDEs arising in the formation of liquid drop pattern using Sumudu transform based technique, Partial Differ. Equ. Appl. Math. 8 (2023) 100578.
[40] Z.U.A. Zafar, S. Zaib, M.T. Hussain, C. Tunç, S. Javeed, Analysis and numerical simulation of tuberculosis model using different fractional derivatives, Chaos Solitons Fractals 160 (2022) 112202.
[41] F.T. Akyildiz, F.S. Alshammari, Complex mathematical SIR model for spreading of COVID-19 virus with Mittag-Leffler kernel, Adv. Differ. Equ. 2021 (1) (2021) 319.
[42] Y.M. Rangkuti, S. Side, M.S.M. Noorani, Numerical analytic solution of SIR model of Dengue fever disease in south Sulawesi using homotopy perturbation method and variational iteration method, J. Math. Fundam. Sci. 46 (1) (2014) 91–105.
[43] S. Man-Keung, The role of M (mathematical worlds) in HPM (history and pedagogy of mathematics) and in STEM (science, technology, engineering, mathematics), ZDM–Math. Educ. 54 (7) (2022) 1643–1655.
[44] S. Rashid, K.T. Kubra, H. Jafari, S.U. Lehre, A semi-analytical approach for fractional-order Boussinesq equation in a gradient unconfined aquifers, Math. Methods Appl. Sci. 45 (2) (2022) 1033–1062.
[45] Y. Jawarneh, H. Yasmin, M.M. Al-Sawalha, A. Khan, Numerical analysis of fractional heat transfer and porous media equations within Caputo-Fabrizio operator, AIMS Math. 8 (2023) 26543–26560.
[46] M.I. Syam, M. Al-Refai, Fractional differential equations with Atangana–Baleanu fractional derivative: analysis and applications, Chaos Solitons Fractals X 2 (2019) 100013.
[47] H.M. Srivastava, Fractional-order derivatives and integrals: introductory overview and recent developments, Kyungpook Math. J. 60 (1) (2020) 73–116.
[48] A. Atangana, I. Koca, Chaos in a simple nonlinear system with Atangana–Baleanu derivatives with fractional-order, Chaos Solitons Fractals 89 (2016) 447–454.
[49] Z.M. Odibat, N.T. Shawagfeh, Generalized Taylor's formula, Appl. Math. Comput. 186 (1) (2007) 286–293.
[50] N.H. Sweilam, S.M. Al-Mekhlafi, D. Baleanu, Optimal control for a fractional tuberculosis infection model including the impact of diabetes and resistant strains, J. Adv. Res. 17 (2019) 125–137.
[51] C. Coll, A. Herrero, E. Sánchez, N. Thome, A dynamic model for a study of diabetes, Math. Comput. Model. 50 (5–6) (2009) 713–716.
[52] Z.U.A. Zafar, Application of $\mathcal{ZZ}$ transform method on some fractional differential equations, Int. J. Adv. Eng. Glob. Technol. 4 (2016) 1355–1363.
[53] D. Baleanu, A. Fernandez, On some new properties of fractional derivatives with Mittag-Leffler kernel, Commun. Nonlinear Sci. Numer. Simul. 59 (2018) 444–462.
[54] S. Rashid, F. Jarad, H. Alamri, New insights for the fuzzy fractional partial differential equations pertaining to Katugampola generalized Hukuhara differentiability in the frame of Caputo operator and fixed point technique, Ain Shams Eng. J. 15 (54) (2024) 102782.
[55] J. Biazar, H. Ghazvini, Convergence of the homotopy perturbation method for partial differential equations, Nonlinear Anal., Real World Appl. 10 (5) (2009) 2633–2640.
[56] J.H. He, Homotopy perturbation technique, Comput. Methods Appl. Mech. Eng. 178 (3–4) (1999) 257–262.
[57] M. Ma, S. Liu, J. Li, Does media coverage influence the spread of drug addiction?, Commun. Nonlinear Sci. Numer. Simul. 50 (2017) 169–179.
[58] J. Yang, L. Wang, Global dynamical analysis of a heroin epidemic model on complex networks, J. Appl. Anal. Comput. 6 (2) (2016) 429–442.
[59] G.A. Gottwald, I. Melbourne, The 0–1 test for chaos: a review, in: Chaos Detection and Predictability, 2016, pp. 221–247.
[60] S.M. Pincus, Approximate entropy as a measure of system complexity, Proc. Natl. Acad. Sci. 88 (1991) 2297–2301, https://doi.org/10.1073/pnas.88.6.2297.
[61] S. En-hua, C. Zhi-jie, G. Fan-ji, Mathematical foundation of a new complexity measure, Appl. Math. Mech. 26 (2005) 1188–1196, https://doi.org/10.1007/bf02507729.